A Platinum Open Access Journal for Organic Chemistry

Review

Free to Authors and Readers | DOAJ Seal | *Arkivoc* **2024** (6) 202412303

Diazadiborinines and related compounds: a review

José Elguero and Ibon Alkorta*

Instituto de Química Médica, CSIC, Juan de la Cierva, 3, E-28006 Madrid, Spain
Email: ibon@iqm.csic.es

Received 10-09-2024 **Accepted** 11-27-2024 **Published on line** 12-31-2024

Abstract

This review summarizes the content of most publications reporting diazadiborinines and related compounds of the triel group (Al, Ga and In). After a first part describing the synthetic methods, the reactivity of these systems is discussed with special stress on two problems: the equilibrium and isomerism between 1,4 and 1,3-species. ^{11}B NMR data are discussed in relation to the preceding problems. Finally, all the X-ray structures reported in the Cambridge Structural Database are reported and analyzed.

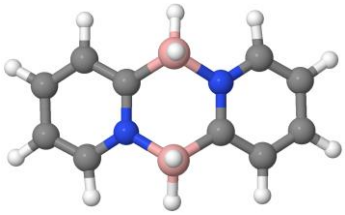

1,4

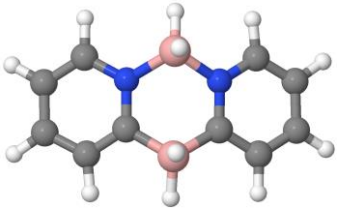

1,3

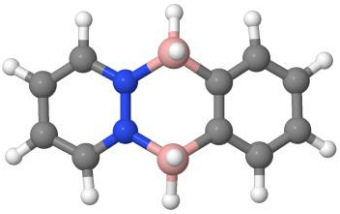

1,2

Keywords: Azaboles, diazaborinanes, dipyridinodiboron, pyridazinediboron, triel group, 'ring-flipping´ mechanism, ^{11}B NMR, X-ray structures.

Table of contents

1. Introduction

6-6-6 Tricyclic compounds with the lateral rings belonging to the azine series and the central one containing two atoms of the triel group (T) are related to azaboles an important class of compounds (Scheme 1).[1-3] Azaboles are obtained by dimerization of azolylboranes and similarly dipyridodiazadiborinines of the *para* class ***a*** (bottom, left) are obtained by dimerization of 2-boraneylpyridines ***m***, both species being in equilibrium.

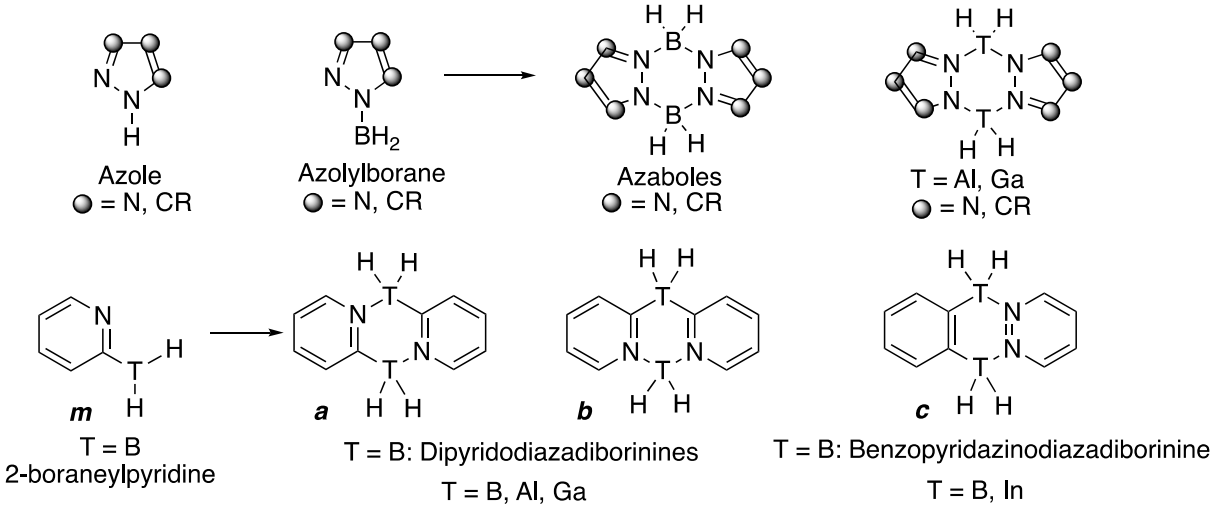

Scheme 1. Boron derivatives, azaboles and diazadiborinines (T = B) as well as their aluminium (T = Al), gallium (T = Ga) and indium (T = In) analogs.

Although the number of possible structures of the 6-6-6 tricyclic compounds is very large depending on the position of the N atoms only three kinds are known with two nitrogen atoms in *para* ***a***, *meta* ***b*** (pyridines) and *ortho* positions ***c*** (pyridazines). In terms of nomenclature, we propose a three letters followed by a number code, Figure 1:

1) elements **B**, **Al**, **Ga**, **In** (**T**, triel group, for any of them).

2) The diazaborinane code ***a*** [**1,4**,2,5], ***b*** [**1,3**,2,5], ***c*** [**1,2**,3,6] (Scheme 2).

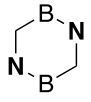

[**1**,**4**,2,5] ***a***

$1\lambda^2,4\lambda^2,2\lambda^2,5\lambda^2$-diazadiborinane

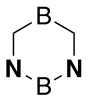

[**1**,**3**,2,5] ***b***

$1\lambda^2,3\lambda^2,2\lambda^2,5\lambda^2$-diazadiborinane

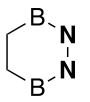

[**1**,**2**,3,6] ***c***

$1\lambda^2,2\lambda^2,3\lambda^2,6\lambda^2$-diazadiborinane

Figure 1. The 1,4, 1,3 and 1,2-diazadiborinanes.

3) A number for the type of substituents on the boron atoms and on the pyridine (or pyridazine) rings. For instance, in the most common **B** series the three unsubstituted diazadiborinines (T = B) of Scheme 1 are **B*a*1**, **B*b*1** and **B*c*1** while the monomer is **B*m*1**. They have the same formula, $C_{10}H_{12}B_2N_2$, while that of the monomer is the half, C_5H_6BN. Note that **B*a*1**, **B*b*1**, **B*c*1** and **B*m*1** are unknown.

In Figure 2 are reported some data about correct nomenclature and atom numbering.

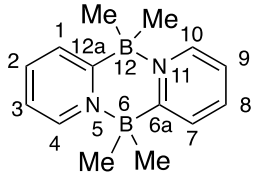

B*a*

6,6,12,12-tetramethyl-6,12-dihydro-$5\lambda^4,6\lambda^4,11\lambda^4,12\lambda^4$-dipyrido[2,1-*c*:2',1'-*f*][1,4,2,5]diazadiborinine
Tetramethylbis[2-pyridinyl-κ(C;κN)]diboron

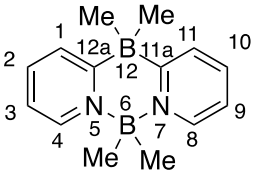

B*b*

6,6,11,11-tetramethyl-6,11-dihydro-$5\lambda^4,6\lambda^4,11\lambda^4,12\lambda^4$-benzo[*d*]pyrido[1,2-*a*][1,3,2,5]diazadiborinine
Tetramethyl[μ-(2-pyridinyl-C^2:N^1)diboron

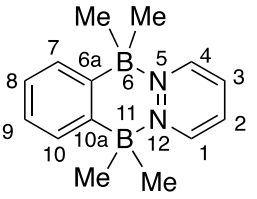

B*c*

6,6,11,11-tetramethyl-6,11-dihydro-$5\lambda_4,6\lambda_4,11\lambda_4,12\lambda_4$-benzo[*d*]pyridazino[1,2-*a*][1,2,3,6]diazadiborinine
Tetramethyl[μ-(pyridazine-κN^2:κN^3)diboron

Figure 2. Atom numbering and names for the tetramethyl derivatives.

4) Finally, a correlative number, from **1** to **19** was used after the three letters to differentiate the compounds with the same letter's code.

Related to the present review there are two rolling reviews covering related families of polycyclic boron compounds that would be useful to cite.[4,5]

2. Synthesis

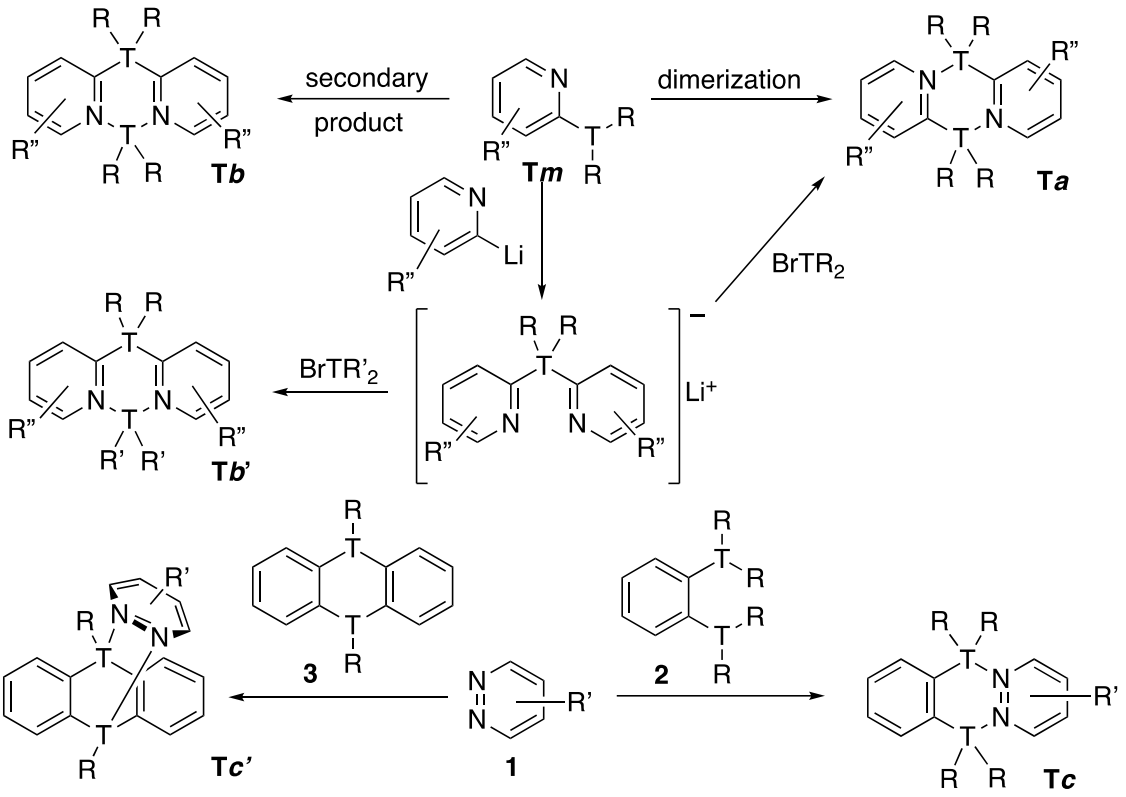

Scheme 2. Synthetic methodologies. R, R', R" are different substituents.

The three kinds of structures are different from the synthetic point of view, Scheme 2. **T*a*** series are the dimers of 2-TR_2-pyridines (**T*m***), a barrierless equilibrium whose position depends on the substituents. **T*b*** series appear accidently in some of the previous syntheses; besides, there is a known method to prepare them specifically allowing to have two different substituents, R and R', on the T = B atoms, **T*b*'** (see Scheme 3, compound **B*b*3**) The synthesis of **T*c*** compounds corresponds to two procedures, that on the right side **T*c*** results from the reaction between **1** and **2**, is the less common but affords compounds of similar geometry than the preceding ones; that on the left side **T*c*'** starts from 5,10-dihydroboranthrene (**3**, T = B) that forms complexes with pyridazine, phthalazine, cinnoline and benzo[*c*]cinnoline (**1**). These complexes have a trypticene form (Figure 3).

The syntheses will be discussed in chronological order, although in some cases, recent publications reference older synthetic procedures, which may alter the sequence. The results reported in references [6] and [7] are summarized in Scheme 3.

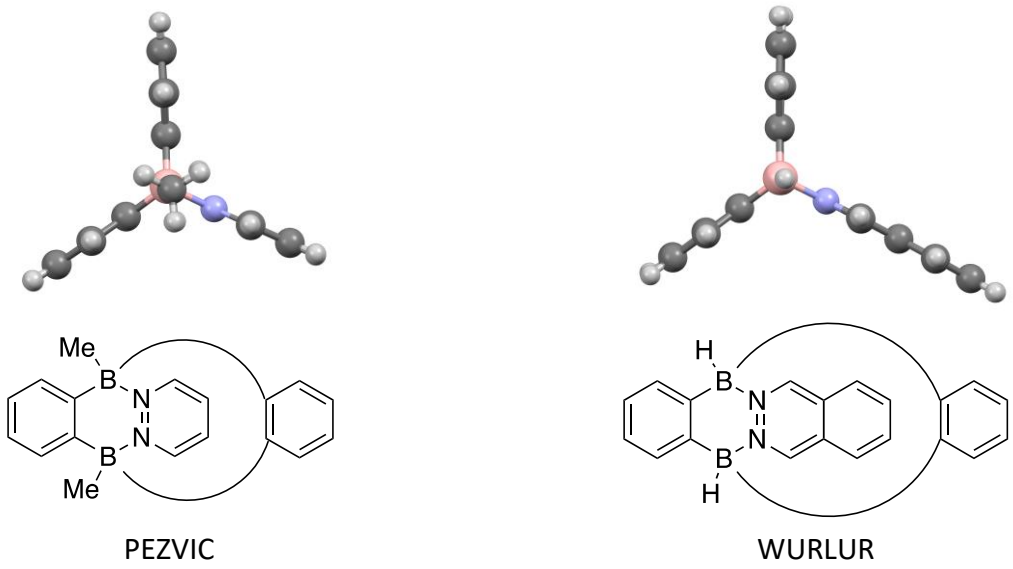

Figure 3. The X-ray structures of two diazadiboratrypticenes, for the PEZVIC and WURLUR CSD refcodes see section 5. Solid-state properties.

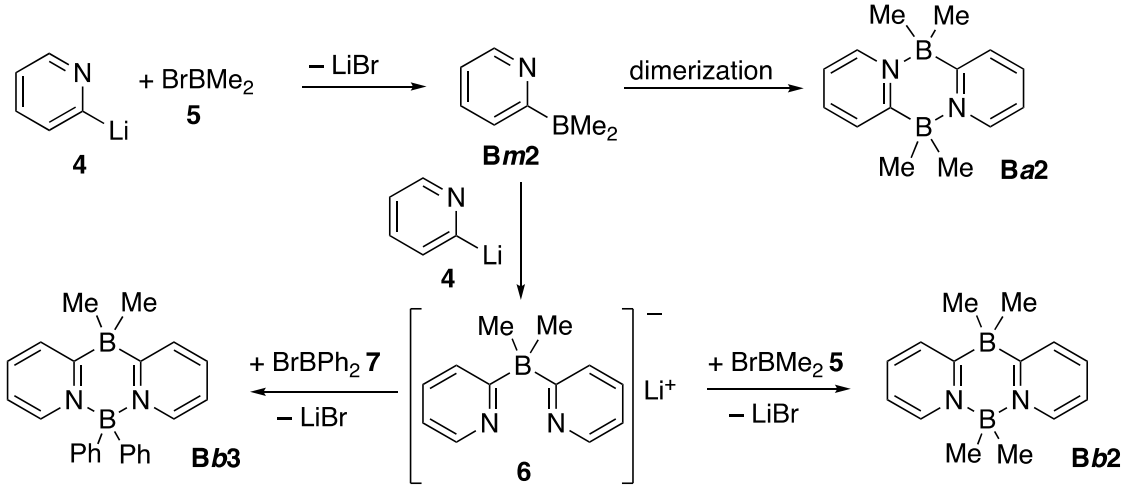

Scheme 3. Synthesis of B***m*2**, B***a*2**, B***b*2** and B***b*3**.

The compounds shown in Scheme 3 are obtained from bromodimethylborane (**5**) and 2-lithiopyridine (**4**) at low temperatures.[6,7] This reaction produces four chromatographic fractions. The third and fourth fractions, obtained with a yield of 50%, were mixtures of B***a*2** (*Tetramethylbis[2-pyridinyl-*κ*(C;*κ*N)]diboron*) and B***b*2** (*Tetramethyl[*μ*-(pyridazine-*κ*N2:*κ*N3)diboron*) in a ratio of 15:85, respectively, as determined by preparative thin-layer chromatography (TLC) and ^{1}H NMR. The only known example of an asymmetric compound in the ***b*** series, B***b*3**, was prepared according to Scheme 3 using bromodiphenylborane (**7**) instead of bromodimethylborane (**5**).

Scheme 4 summarizes the results from reference.[8]

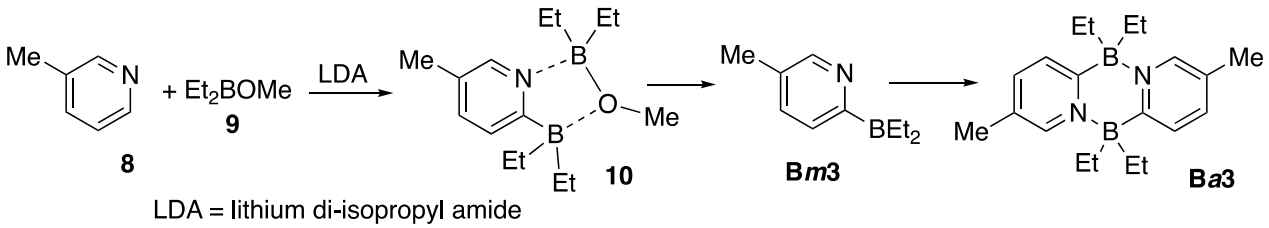

Scheme 4. Synthesis of **B*m*3** and **B*a*3**. A dimer **B*a*3'**, lacking methyl groups, was also synthesized.

The main challenge in the procedure outlined in **Scheme 4** lies in the synthesis of compound **10**. Although 2-lithiopyridines are available *via* a low-temperature halogen-metal exchange it is known that Martin *et al*.[9] demonstrated that direct 2-lithiation of pyridines takes place effectively with sterically hindered bases in the presence of reagents having the ability to coordinate with the nitrogen atom of pyridines. In order to introduce a boryl group at the 6 position of 3-methylpyridine (**8**), the authors of reference[8] applied the Martin method, that is, lithiation with lithium diisopropylamide (LDA) at –78 °C in ether in the presence of diethylmethoxyborane (**9**). ^{1}H NMR spectrum showed signals due to four ethyl groups and the pyridine skeleton (compound **10**). Heating of the material at 180 °C under 20 mmHg gave **B*m*3**. This compound spontaneously dimerizes to **B*a*3**.

The diindacycle **1In*c*1** was prepared according to the procedure reported in Scheme 5.[10]

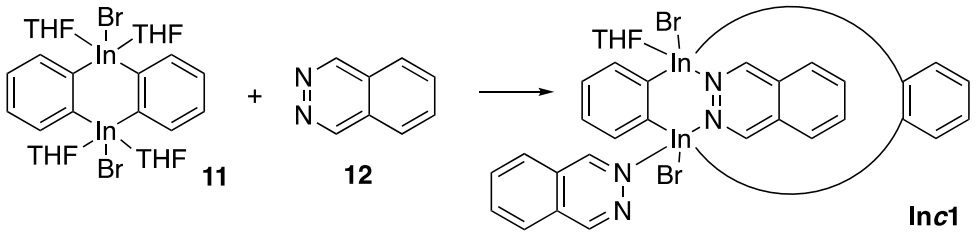

Scheme 5. Synthesis of **In*c*1**.

While the 1:4 complex (1)-phthalazine:(4)THF (**11**) appears to be the preferred species in solution, colorless pale-yellow crystals of the less soluble 1:2 complex 1-2(phthalazine)·THF **In*c*1** spontaneously formed in a saturated THF solution containing equimolar amounts of **11** and phthalazine (**12**). Compound **In*c*1** crystallizes in the monoclinic space group. As shown in Scheme 7, the diindacycle **11** acts as a ditopic receptor for one phthalazine molecule.

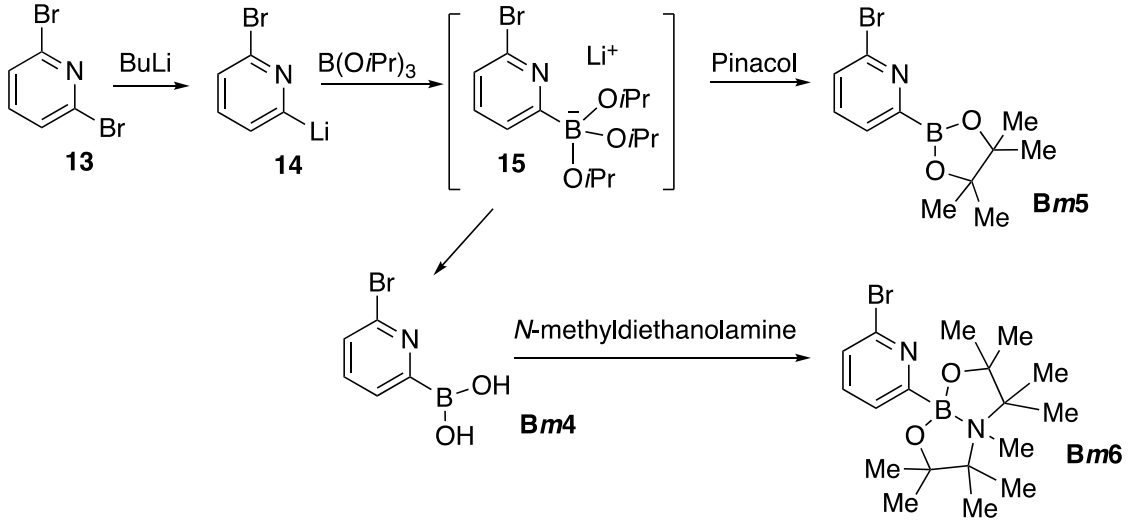

Scheme 6. Synthesis of **B*m*4**, **B*m*5** and **B*m*6**.

The X-ray structures of **B*m*5**[11] and **B*m*6**[12] (Scheme 6) were the first reported structures of stable monomers (see section 5). They were synthesized from 2,6-dibromopyridine (**13**) using the method developed by Bouillon *et al*.[13] Boronic acid pinacol ester **B*m*5** and dioxazaborocane **B*m*6** were obtained from 2,6-dibromopyridine (**13**) through intermediates **14**, **15**, and **Bm4**.[13] Other related compounds were also prepared.

The synthesis of four aluminium derivatives from **Al*a*1** to **Al*a*4** is summarized in Scheme 7, along with an example of their reactivity in the formation of **16**.[14] The reaction of $[Cp^*Al]_4$ with RR'_2SiN_3 in refluxing toluene in the presence of an equimolar amount of DMAP proceed with N_2 elimination. Dark-colored solutions form, from which colorless crystals of dihydroanthracene-type compounds of the general type **Al*a**n*** (n = 1, 2, 3, 4) are isolated after storage at –60 °C. These compounds also form when DMAP-stabilized iminoalanes were heated in toluene at 110 °C for 1 h. **Al*a*3** reacts with DMAP to yield **16** (see section 3. Reactivity and the monomer/dimer problem).

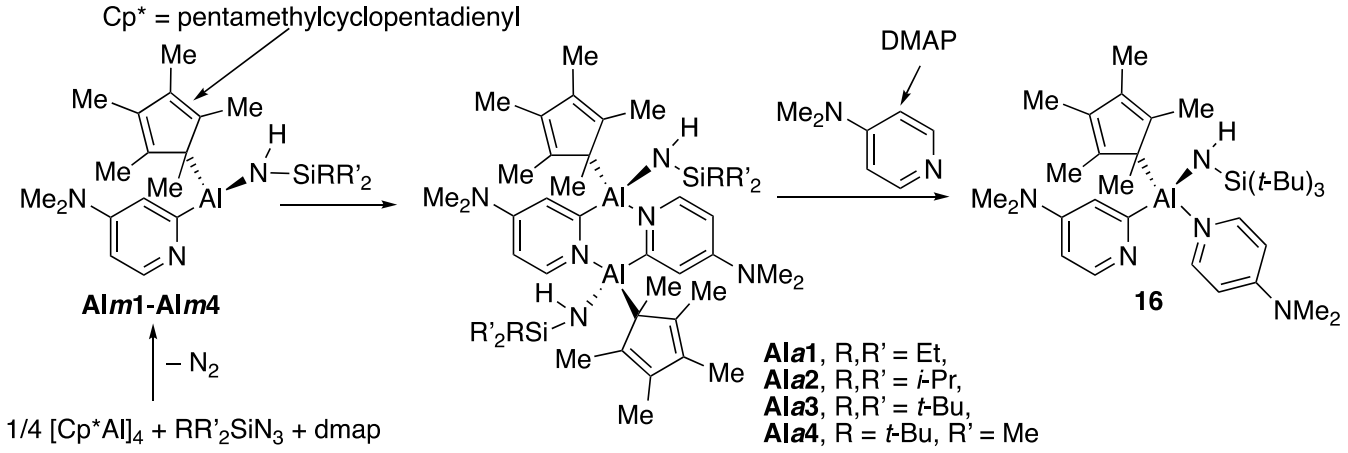

Scheme 7. Synthesis of **Al*a*1**, **Al*a*2**, **Al*a*3** and **Al*a*4**.

The dimers of Scheme 8, whose structures were published in 2007 by Wright *et al*.[15] were prepared using methodologies reported in the previous references [6] and [7] by Hodgkins *et al*. The **Al** isomers were obtained from a low-temperature reaction of $ClAlMe_2$ (**17**) with 2-lithium-pyridine (**4**) in 56% yield. The presence of the two isomers **Al*a*5** and **Al*b*5** in *ca*. 50:50 ratio was confirmed by ^{1}H NMR. These NMR observations are similar to those reported previously for the *ca*. 15:85 mixture of **B*a*2** and **B*b*2** (Scheme 3). Since the starting material Me_2GaCl (**20**) is difficult to synthesize, the gallium compound **20** was prepared by the *in-situ* reaction of $GaCl_3$ (**19**) with MeLi (1:2 equiv., respectively) followed by reaction with 2-litium-pyridine (**4**) (28% yield). In contrast to the related B and Al compounds, only trace amounts of the 1,3-isomer **Ga*b*5** could be detected in the *in situ* ^{1}H NMR spectrum of the reaction mixture, with the isolated crystalline product being exclusively the 1,4-isomer **Ga*a*5**.

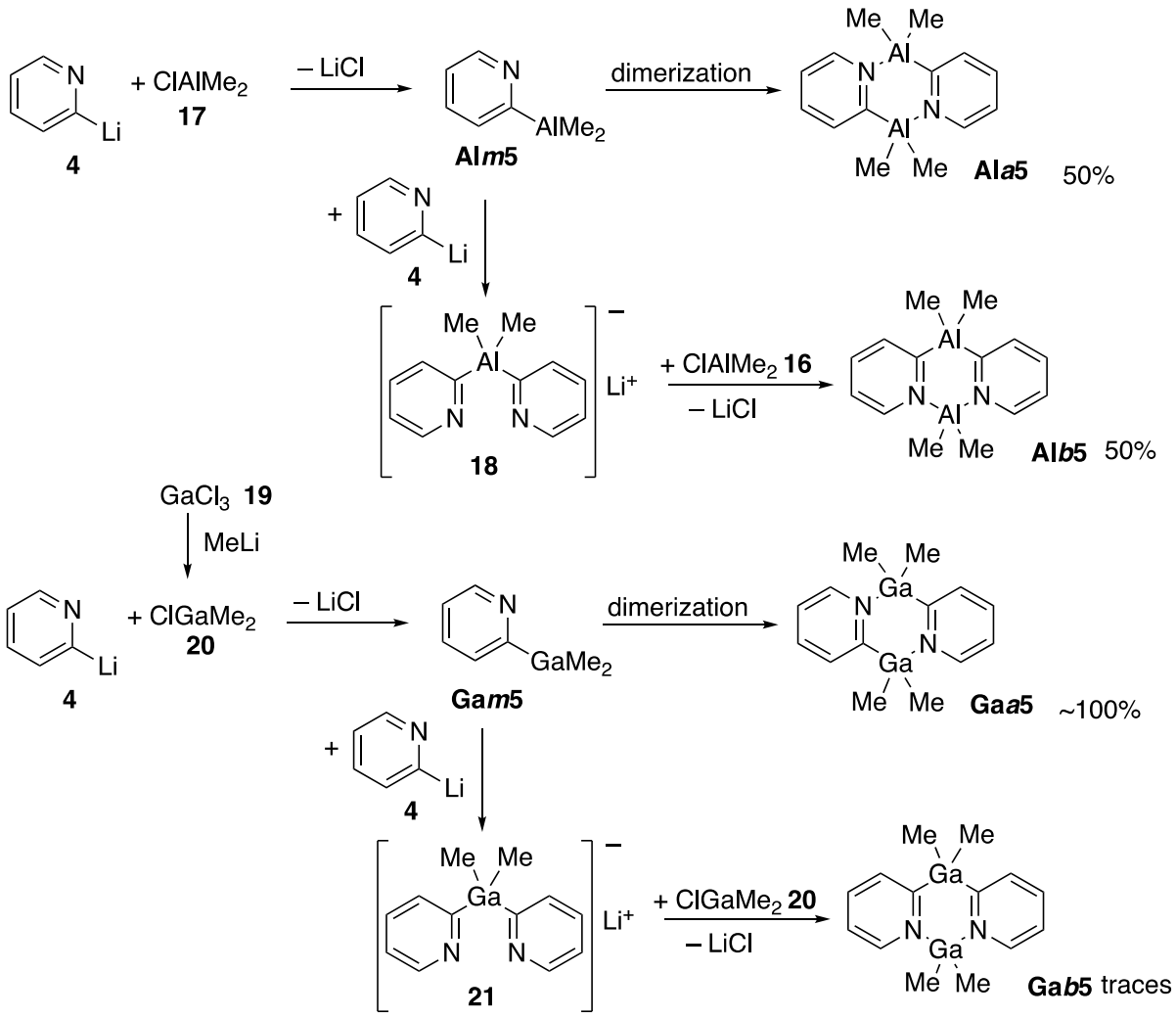

Scheme 8. Synthesis of **Al*m*5**, **Al*a*5**, **Al*b*5**, **Ga*m*5**, **Ga*a*5** and **Ga*b*5**.

In 2024 Wright *et al*. prepared five more aluminium derivatives (**Al6**, **Al7**, **Al8**, **Al9** and **Al10**) using the same method and determined their X-ray structures (see Section 5. Solid-state properties: X-ray crystallography). They also investigated the **a**/**b** interconversion mechanism (see Section 3. Reactivity and the monomer/dimer problem) Figure 4.[16]

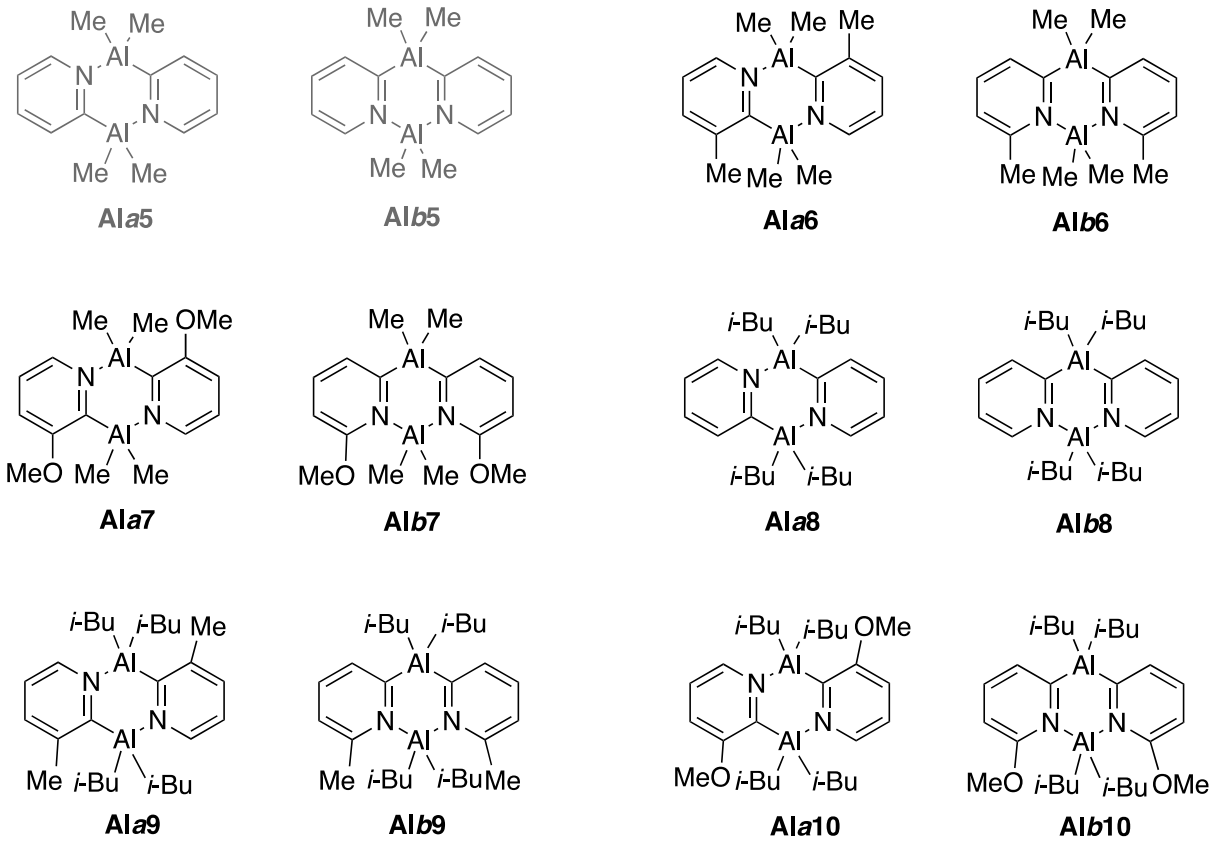

Figure 4. Isomerism **a**/**b** in aluminium derivatives including **Al*a*5** and **Al*b*5** from Scheme 8.

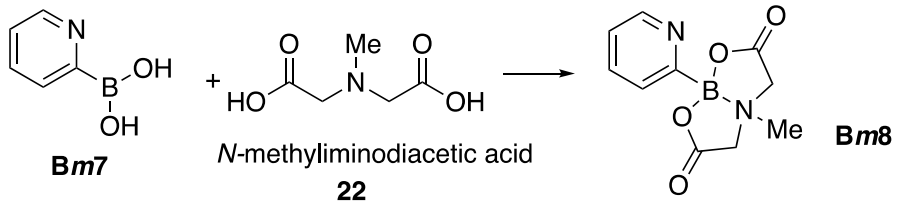

Scheme 9. Synthesis of **B*m*8**.[17,18]

N-Methyliminodiacetic acid (MIDA, **22**) reacts with **B*m*7** to form the boronate **B*m*8**, which represent the first air-stable source of boronic acids by virtue of their stability and remarkable capacity for *in situ* slow release of unstable boronic acids.[17,18]

Pentafluoropyridine (**23**) was catalytically converted into its 2-boryl derivative **B*m*9** with a 45% yield in the presence of a rhodium catalyst as shown in Scheme 10. This represents the first example of catalyzed borylation of a C–F bond.[19]

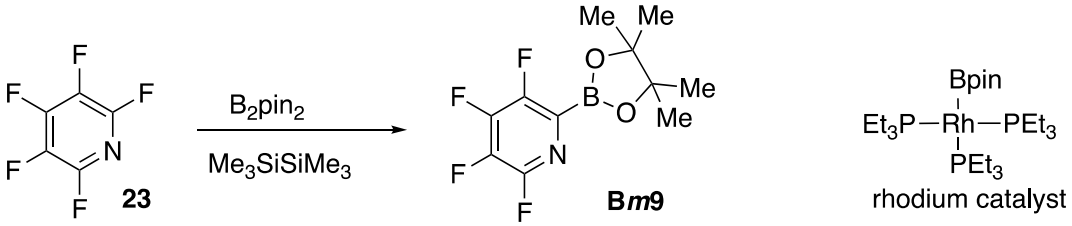

Scheme 10. Synthesis of **B*m*9**.

When the DMS adduct **24** was treated with pyridazine **1** and phthalazine **12**, compounds **Bc1** and **Bc2** were obtained, as depicted in Scheme 11.[20]

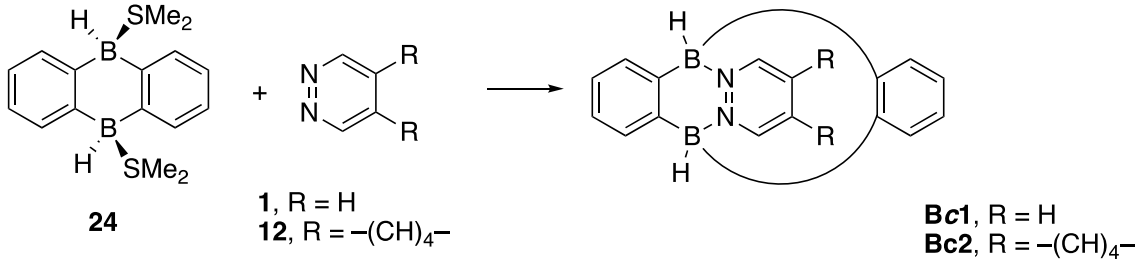

Scheme 11. Synthesis of **Bc1** and **Bc2**.

The results reported in reference[21] are rich in information (Scheme 12). Regarding the synthesis of monomer/dimer couples, **B10** and **B11** start from 2-bromoaniline and follow the sequence **25** → **26** (*N*-allyl-*N*-methyl-2-bromoaniline) → **27** (*N*-vinyl aniline, *E/Z* > 19:1) + reaction with **28** (1-chloro-*N*,*N*-diisopropyl-1-vinylboranamine) → **29** → **30** (mono-benzo-fused 1,4-azaborine) → **31**. From this last compound, the use of 2-lithiumpyridine (**4**) or 2-lithium-6-methylpyridine (**32**) lead to the first or the second series.

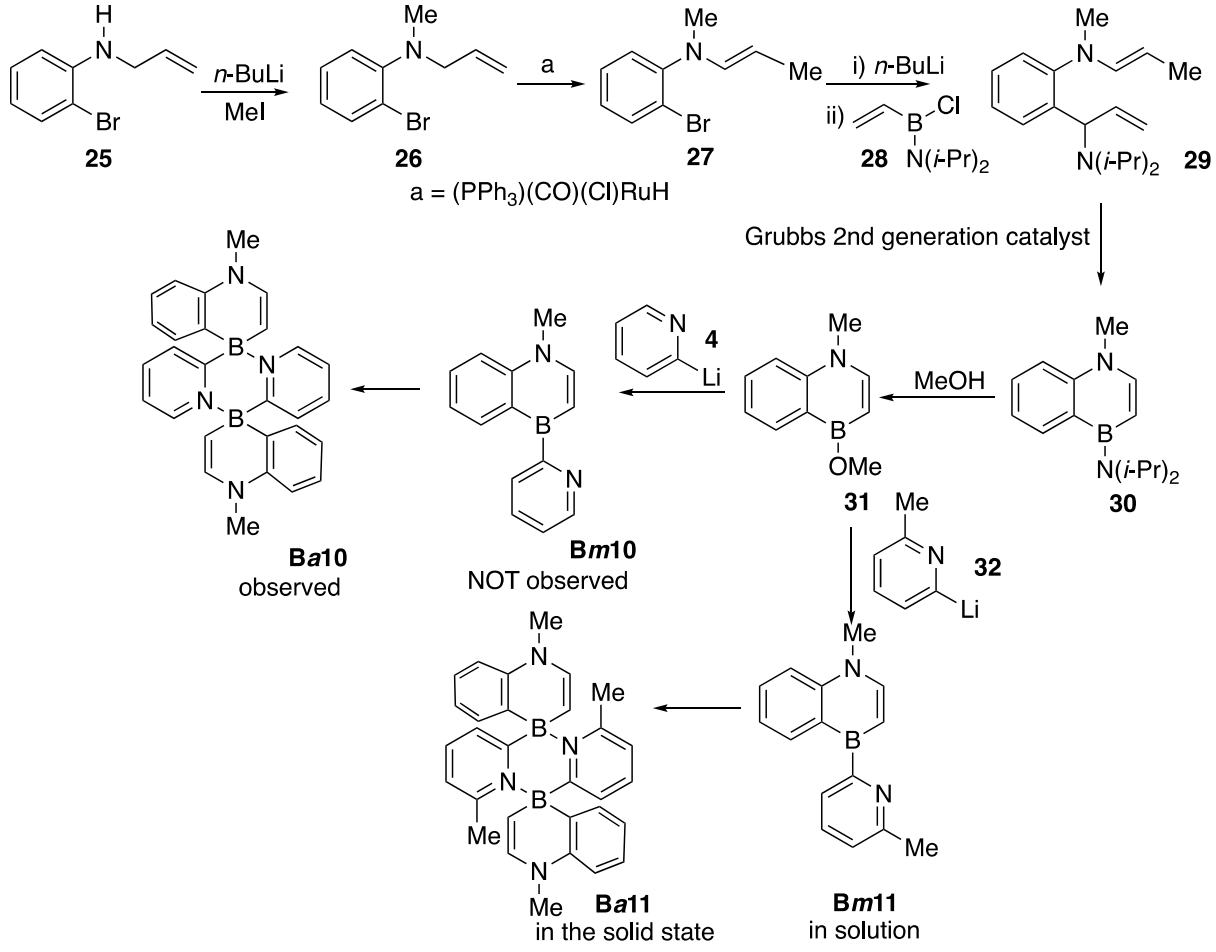

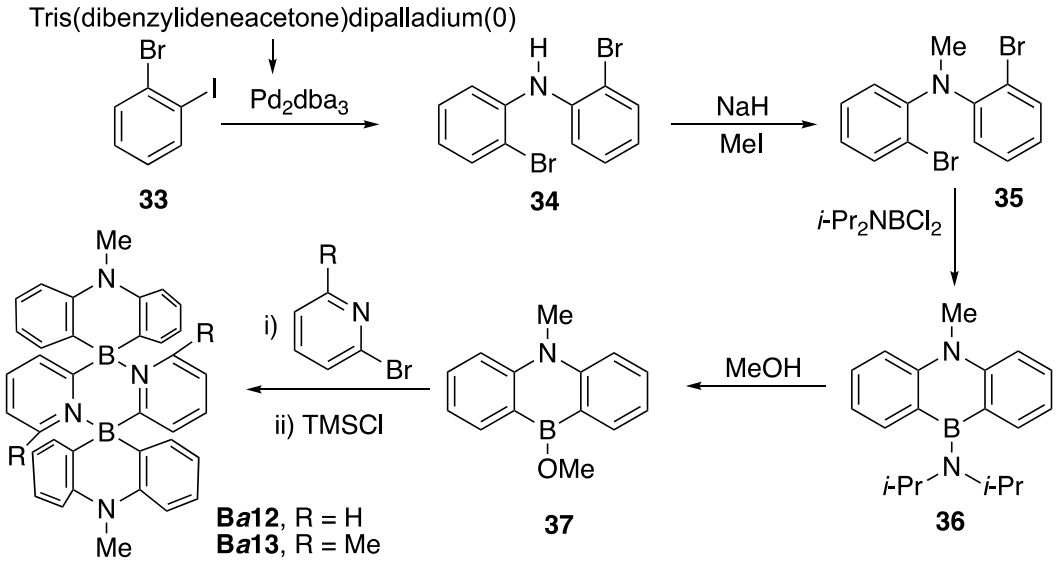

Scheme 12. Synthesis of **B*m*10**, **B*a*10**, **B*m*11**, **B*a*11**, **B*a*12** and **B*a*13**.

The second part of Scheme 12 is to be found in the Supporting Information of the referenced paper.[21] Starting also from 2-bromoaniline and 2-bromoiodobenzene (**33**) the reaction proceeds through intermediates **34**, **35**, **36** and **37**, ultimately yielding **B*a*12** and **B*a*13**, depending on whether 2-bromo or 2-bromo-6-methyl-pyridine is used.

The superbasic, sterically hindered pyridine ligand **B*m*13** was synthesized according to Scheme 13.[22]

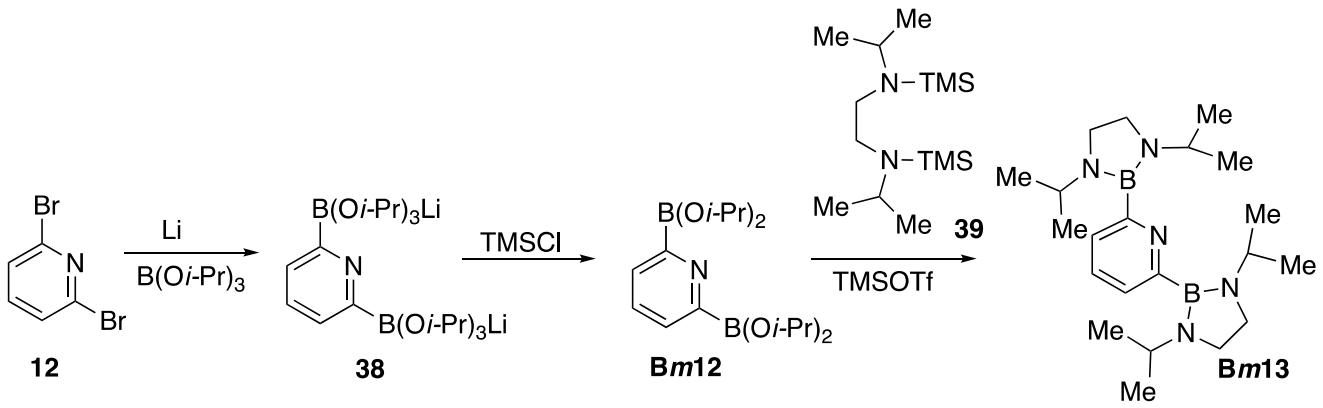

Scheme 13. Synthesis of **B*m*12** and **B*m*13**.

The synthesis of the symmetrical pyridyl boronic acid ester **B*m*12** is quite complex. Since the di-lithiation of 2,6-dibromopyridine (**12**) with nBuLi proved problematic, it was replaced by a one-pot synthesis with elemental lithium (Scheme 13). When lithium was introduced into a solution of 2,6-dibromopyridine in the presence of B(O*i*-Pr)$_3$ in THF at –30 °C, a slurry mixture of **38** was formed. The solvent was replaced with CH_2Cl_2 and treatment with TMSCl immediately led to the immediate formation of a colorless precipitate. The reaction mixture was heated to reflux for 24 h to complete the transformation. After workup, fractional distillation gave the symmetrical pyridyl boronic acid ester **B*m*12** with an overall yield of 45%.

Readily available *N,N'*-bis(isopropyl)-*N,N'*-bis(trimethylsilyl)-1,2-ethanediamine (**39**) was added to a hexane solution of **2**, with a catalytic amount of TMSOTf (trimethylsilyl trifluoromethanesulfonate). After

heating the reaction mixture to reflux for 12 hours, the reaction proceeded quantitatively, as confirmed by multinuclear NMR spectroscopy. **B*m*13** was isolated as a colorless crystalline solid in 94% yield.

A new compound of the ***c*** series was synthesized, as shown in Scheme 14.[23] The bisborane **40**, undergoes Lewis pair coordination with benzo[*c*]cinnoline (**41**) to yield **B*c*3.**[23]

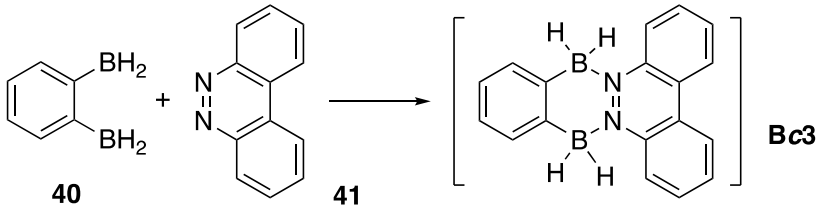

Scheme 14. Synthesis of **B*c*3**.

Another important contribution of Wegner to this field is the synthesis of **B*c*4**,[24] which is formed by reacting of 1,2-bis(trimethylsilyl)benzene (**42**) and pyridazine (**1**), according to Scheme 15, to afford the bisboron–pyridazine complex **B*c*4**.

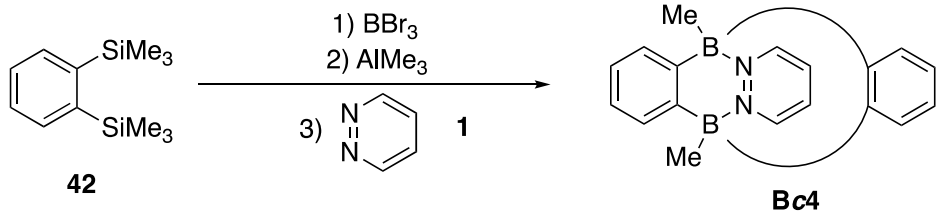

Scheme 15. Synthesis of **B*c*4**.

In Scheme 16, 5,10-dichloro-5,10-dihydroboranthrene (**43**) was used as starting material. Mixing equimolar amounts of **43** and **1** at 0 °C resulted in a yellow solution corresponding to a 1:1 complex with the **B*c*5** structure.[25]

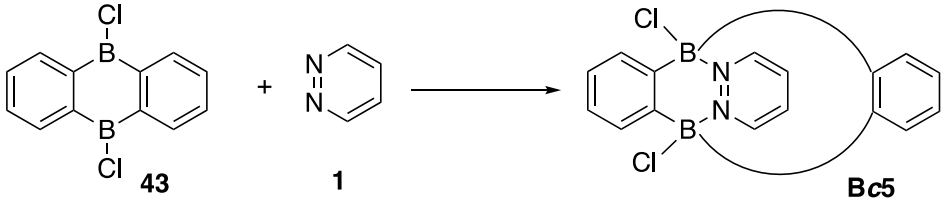

Scheme 16. Synthesis of **B*c*5**.

The reaction of 4,4'-di-*t*-butylpyridine (**44**) with B_2pin_2 [bis(pinacolato)diborane] produces **B*m*14**,[26] as shown in Scheme 17.

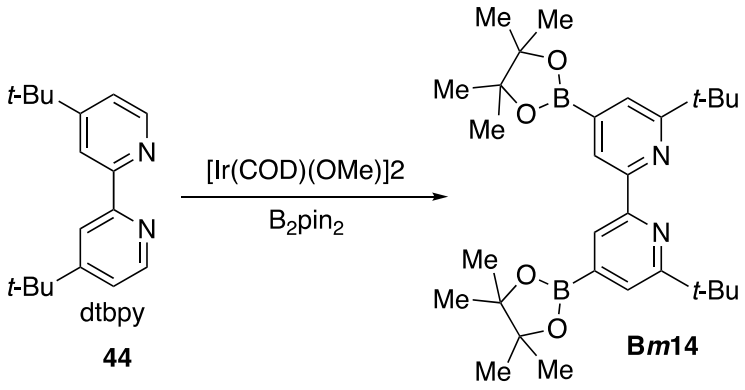

Scheme 17. Synthesis of **B*m*14**.

Almost simultaneously, two similar papers were published. The first one is summarized in Scheme 18,[27] where **B*m*15**, **B*m*16** and **B*m*17** were successfully crystallized.

Yttrium-catalyst **45** was used for *ortho*-selective C–H Borylation of pyridines with pinacolborane HBpin. A very large number of monomers **B*m*** were prepared, and three of them crystalized, but all of them formed dimers (**B*a*15**, **B*a*16** and **B*a*17**).[27]

The second study, summarized in Scheme 19, involves the organolanthanide (**47**)-catalyzed C−H α-mono-borylation of pyridines.[28] Several pyridines were used in the study, and fortunately, the dimers (**B*a*18** and **B*a*19**) formed were different (see Section 5. Solid-state properties: X-ray crystallography).

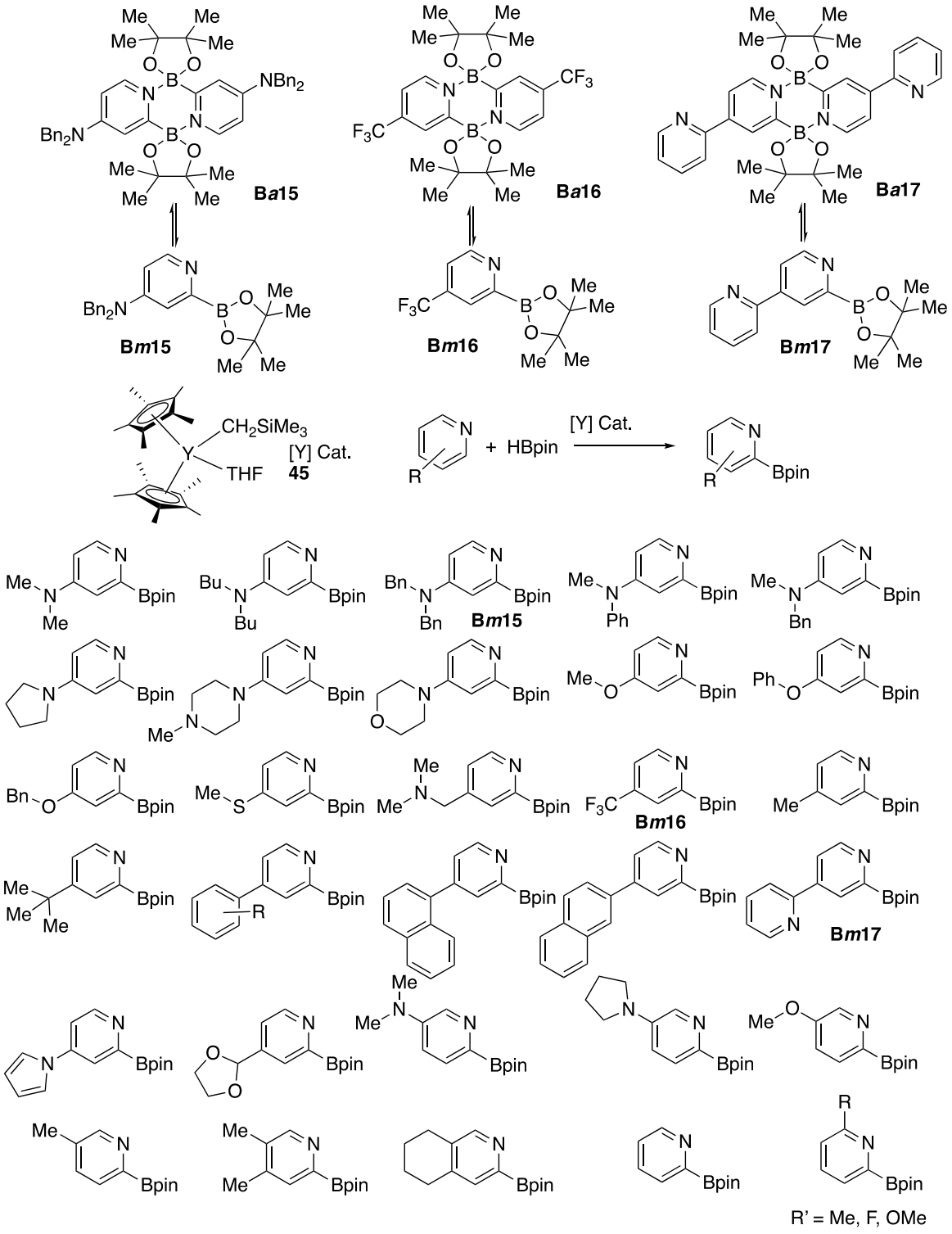

Scheme 18. Synthesis of **B*a*15**, **B*a*16**, **B*a*17**, **B*m*15**, **B*m*16** and **B*m*17**.

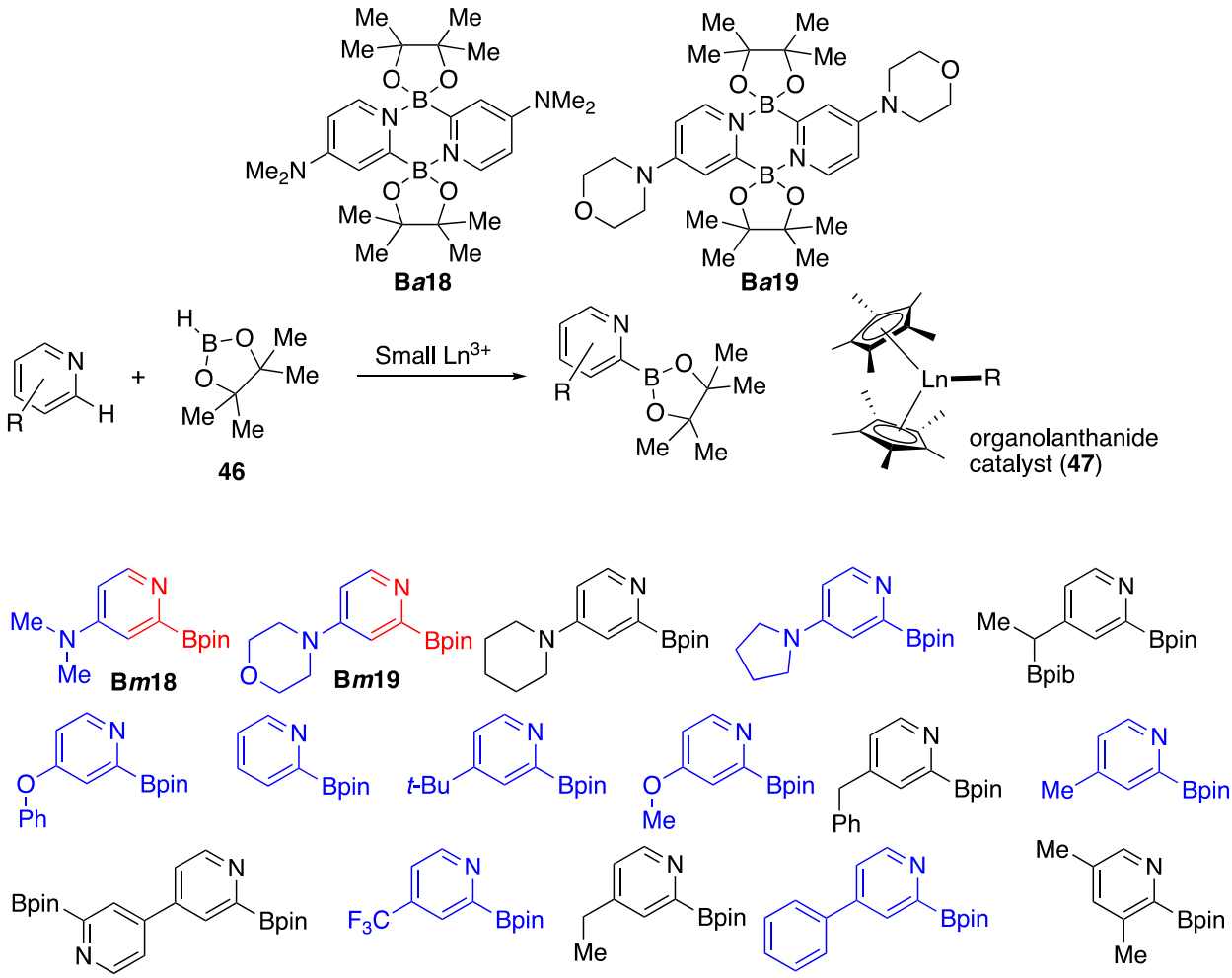

Scheme 19. Synthesis of **B*a*18** and **B*a*18**. In blue common with [27]; in red, X-ray dimers.

3. Reactivity

3.1 The monomer (*m*)/dimer (*a*) problem

One of the most important topic concerning the behavior of the compounds discussed in this review is the monomer ***m***/dimer ***a*** equilibrium. In the previous sections, Schemes 3,[7] 4,[8] 7,[17] 8,[15] 11,[21] 17,[27] and 18,[28] are examples of this subject. Typically, this kind of equilibrium is studied in solution by NMR using as independent variables: solvent type, concentration and temperature for compounds with different substituents selected for their electronic and steric variety.[29,30] **These studies are totally absent in diazadiborinines and related compounds**.

In the solid state (as studied by X-ray crystallography; no examples of the use of solid-state NMR are known), these compounds crystallize either as monomers ***m*** or dimers ***a***. In solution, only one species is typically observed by NMR, though small spectroscopic differences between the species make identification challenging. Notably, both species have never been reported to coexist in solution. In one case, a compound exists as a monomer in solution but crystallizes as a dimer in the solid state (see Scheme 21).

Several authors limited their contribution to determine by X-ray crystallography the structure of the resulting compounds either dimers ***a***[6,7,15,27,28] or monomers ***m***[11-13,17,19,22,26] without discussing the

monomer/dimer problem. In many cases, ^{11}B NMR (see section 4. Solution properties: NMR spectroscopy) was employed to confirm the structure in solution.

Murafuji *et al*.[8] reported an interesting experiment, Scheme 20. In a scrambling experiment, the component molecules of reference[8] gave a further support relevant to the marked stability of the dimer. Each dimer composed of **B*m*3** or **B*m*3'** monomers remained unchanged even when equimolar amounts of these dimers **B*a*3** and **B*a*3'** in *p*-xylene-d_{10} were heated at 130 °C for 24 h. No traces of **Ba3"** were detected.

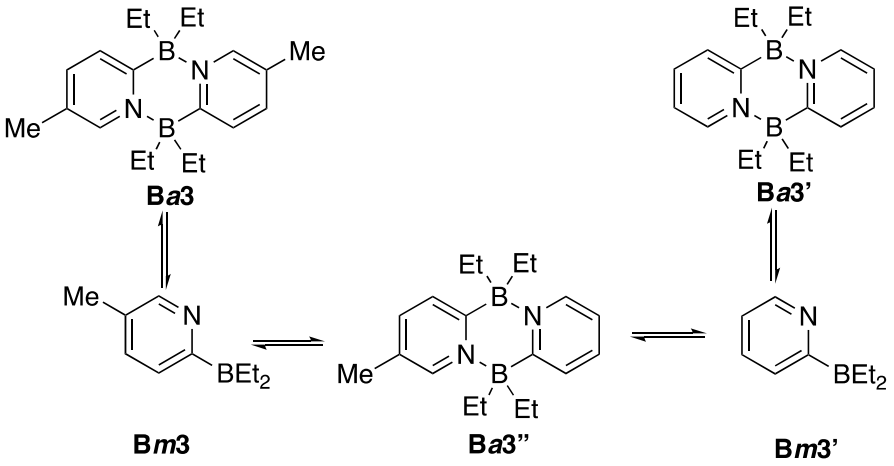

Scheme 20. Murafuji scrambling experiment.

We have summarized Liu *et al*.[21] experiments of Scheme 12 in Scheme 21.

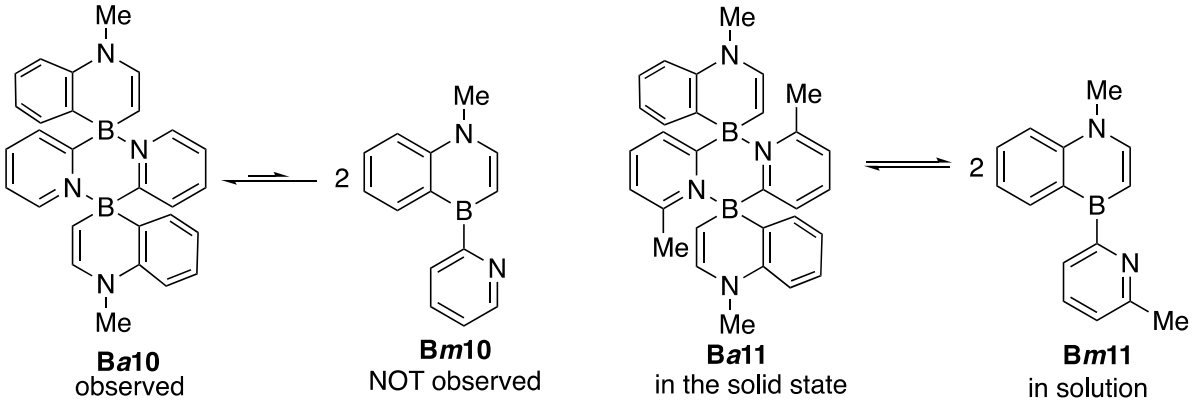

Scheme 21. Monomer/dimer equilibria.[21]

In the **10** series the dimer is more stable than the monomer; the presence of a methyl group at position 6 of the pyridine destabilized the dimer **B*a*11** and both forms are of similar energies to the point that the prevalence of one or the other depends on the phase.

Concerning the reactivity of the dimer in ***a*** series it often went through the less stable monomer ***m***; ring opening being a barrierless mechanism, the reactivity only depends on the difference in energy.

In Scheme 7 the formation of compound **16** (R = R' = *t*-Bu) from **Al*a*3**[14] corresponds, according to the authors to the fact that the strong Lewis base DMAP disaggregates the dihydroanthracene type dimer **Al*a*3**, which can be described as a *head-to-tail* adduct, with subsequent formation of **16**.

3.2 The species (*a*)/1,3 (*b*) isomerism

The results of Schemes 3 and 8 contain a lot of original information on this topic[15] that we have summarized in Figure 5.

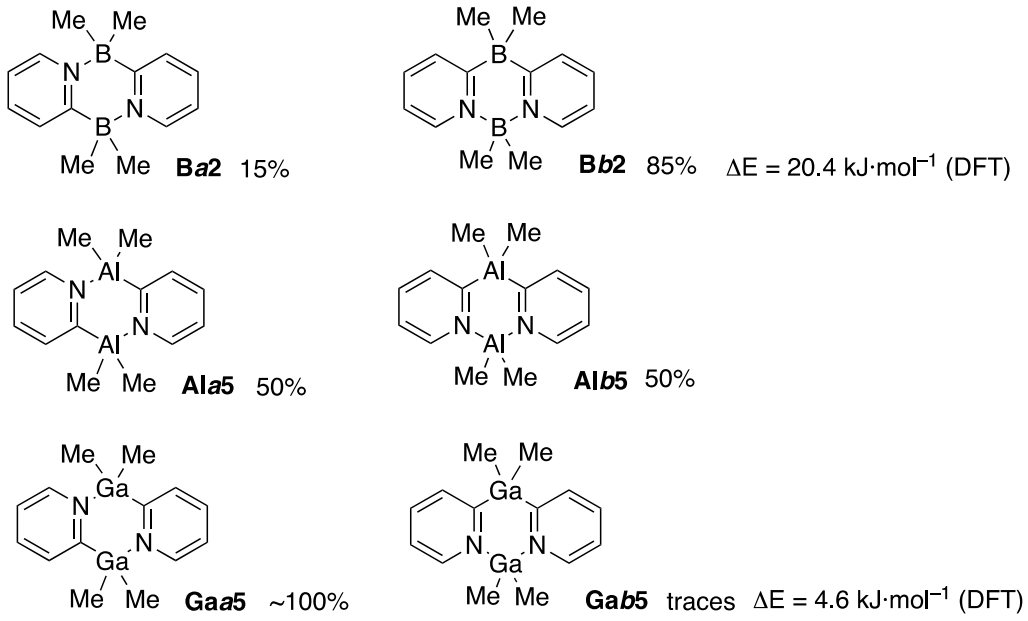

Figure 5. Proportions and differences of energy between ***a*** and ***b*** isomers.

The clear reduction in the amount of the ***b*** isomer as you go down in group 13 of the Periodic Table of the Elements, is consistent with an emerging thermodynamic preference for ***a*** isomers and with there being an accessible activation barrier between the isomers (which decreases as group 13 is descended). Heating a mixture of the isomers **B*a*** or **Al*a*** at reflux for *ca*. 30 min in toluene results in quantitative conversion into **B*a*2** and **Al*a*5** (respectively) as shown by a combination of ^{1}H and ^{11}B NMR spectroscopy. That means that ***a*** isomers are more stable than ***b*** ones, but the 'ring-flipping' mechanism of ***b*** to ***a*** isomerization was not developed.[15]

Seventeen years later, Wright *et al*. revisited the mechanism with a fundamental paper (Scheme 22),[16] where they proposed the 'ring-flipping' mechanism for the compounds of Figure 4. [15] This mechanism accounts for the steric effects of the substituents R' at the 6-position of the pyridine ring. Detailed DFT calculations at the ωB97X-D/6-311++G(d,p)//B3LYP-D3/6-31G(d) level of theory were also reported that will be discussed in section "6. Theoretical calculations". It remains unclear whether this mechanism is applicable to other triel atoms such as B, Ga and In.

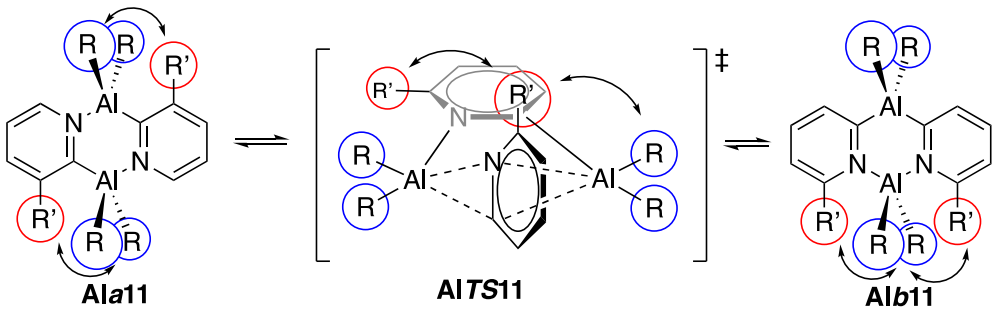

Scheme 22. The 'ring-flipping' mechanism between 1,4 and 1,3-isomers in the **11** series.

3.3 Other reactions

Elimination of hydrogen from **B*c*3** (Scheme 14) leads to the B–N-acene **48** followed by coordination to a second molecule of **41** forming the diradical **49** (Scheme 23.)[23] Both benzo[*c*]cinnoline ligands are chemically equivalent, as implied by their tautomeric forms.

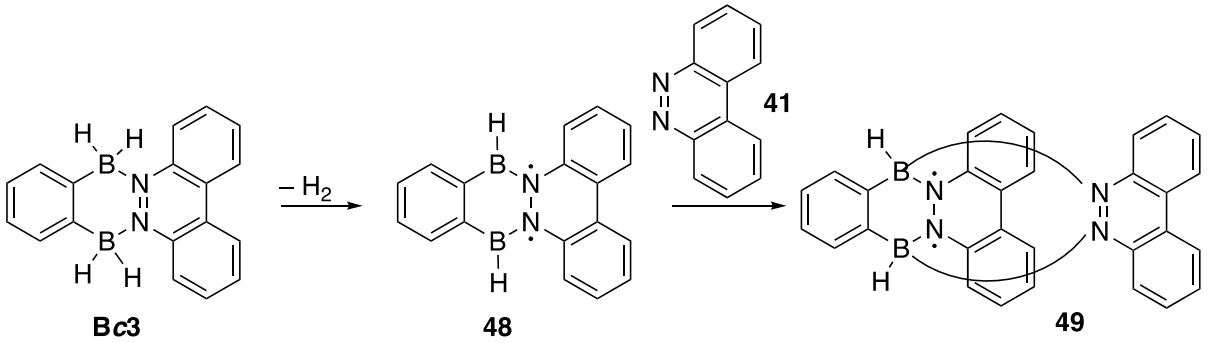

Scheme 23. Reactivity of **B*c*3**.

Treatment of **B*c*5** with TMPZnCl·LiCl (**50**) at 0 °C led to the formation of the zincated pyridazine **B*c*6**. Subsequent iodolysis produces exclusively 4-iodopyridazine (**51**) in 40% yield (Scheme 24).[25]

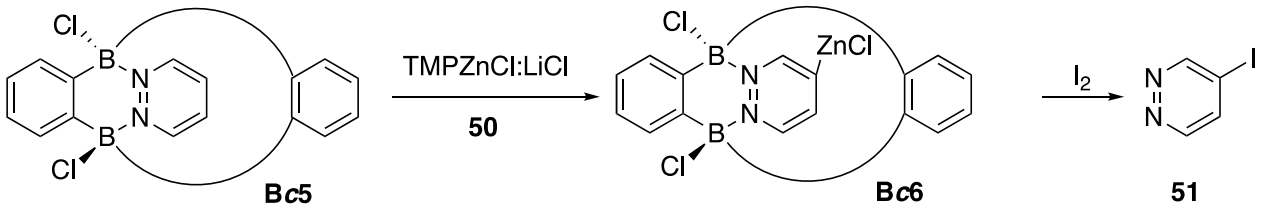

Scheme 24. Synthesis of 4-iodopyridazine from **B*c*5**.

4. Solution Properties: NMR Spectroscopy

There are abundant data concerning ^{1}H and ^{13}C NMR of the compounds of the present review generally as identification tools. More interesting are the abundant ^{11}B (spin 3/2) chemical shifts. A study reports the broad signals of ^{27}Al signals (spin 5/2) of the compounds of Figure 4,[16] though there are no reports of ^{71}Ga NMR (spin 3/2) data. Additionally, the ^{14}N chemical shift of compound **B*a*3** (from Scheme 4) was reported at –137.2 ppm relative to aq. $NaNO_3$ (this old reference is –3.7 ppm from the current nitromethane reference). For this reason, this section will focus on the boron derivatives.

In the case of T = B the four structures of Scheme 1, after adding a substituent, become the structures of Scheme 25.

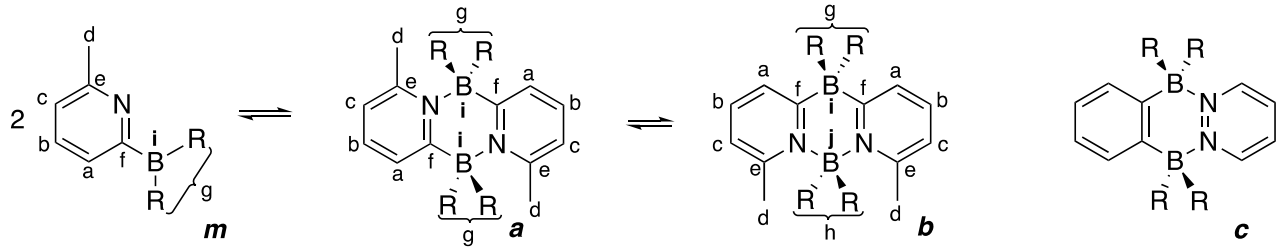

Scheme 25. The four structures of the compounds discussed in this review.

This is an important problem to solve even if there is an X-ray structure in the case of ***m*** and ***a***. Dissolving solid compound can alter the monomer-dimer equilibrium, potentially converting a monomer into a dimer or vice versa.

Structure ***c*** is completely different from a synthetic point of view and cannot be confused with ***a*** and ***b***. In contrast, the three other structures (***m***, ***a*** and ***b***) are in equilibrium, with no barrier between ***m*** and ***a***, but a barrier exists between ***a*** and ***b*** (refer to Scheme 22 and section "6. Theoretical calculations"). There are two methods for differentiating ***a*** and ***b***, one based on their symmetry (which leads to a different number of NMR signals) and the other based on their chemical shifts.

Scheme 25 shows that the number of ^{13}C signals cannot be used to differentiate the three structures (a, b, c, d, e). In ^{1}H NMR structure ***b*** has two BR_2 signals (g, h) while ***a*** has only one (g). The same pattern applies to the number ^{11}B of signals (I, j *vs*. I, respectively). This method cannot be used to distinguish ***m*** (with free BR_2 rotation) from ***a*** (orthogonal R groups).

Table 1 summarizes the information available for the chemical shifts of simple boron derivatives.

Table 1. A summary of chemical shifts with atom letter in brackets

Mol	Nuclei	R	Solvent	Ref.	***m***	***a*** (1,4)	***b*** (1,3)
B2	^{1}H of BR_2	Me	$CDCl_3$	6,7	---	0.22 (g)	0.36 (g) & 0.06 (h)
	^{13}C of BR_2				---	14.9 (g)[a]	14.7 (g & h)
	^{13}C azine ring				---	182 (f)	187 (f)[b]
	^{11}B of BMe_2				---	–5.2 (i)	–17.6 (i) & 3.0 (j)
B3'	^{13}C azine ring	Et	$CDCl_3$	8	---	181.6 (f)	---
	^{11}B of BEt_2				---	–2.30 (i)	---
B3	^{13}C azine ring	Et	$CDCl_3$	8	---	177.8 (f)	---
	^{11}B of BEt_2				---	–2.35 (i)	---
B9	^{11}B of Bpin	Bpin	toluene-d_7	19	28.5 (i)	---	---
B10	^{13}C azine ring	Ring	CD_2Cl_2	21	---	179.5 (f)	---
	^{11}B of Bpin				43 (i)	---	---
B11	^{13}C azine ring	Bpin	CD_2Cl_2	21	168.8 (f)	---	---
B14	^{11}B of Bpin	Bpin	benzene-d_6	26	31.25 (i)	---	---
B15	^{11}B of Bpin	Bpin	$CDCl_3$	27	---	4.6	---
B18	^{11}B of Bpin	Bpin	toluene-d_7	28		5.42	---
B19	^{11}B of Bpin	Bpin	toluene-d_7	28		5.53	---

[a] $^{1}J(^{13}C\text{-}^{11}B)$ = 41.0 Hz, [b] $^{1}J(^{13}C\text{-}^{11}B)$ = 41.0 Hz

Between ***a*** and ***m*** the carbon atom (f) appears at ^{13}C 168.8 (***m***) and 179.5 (***a***). The ^{11}B mean values are ***m*** +34, ***a*** 2, ***b*** –7 ppm.

5. Solid-State Properties: X-Ray Crystallography

The diazadiborinines field has yielded an unusually high number of X-ray structures, which we present in full here. Table 2 and Figure 6 summarizes 27 structures of ***a*** and ***b*** dimers reported to date; corresponding to 16 boron derivatives, nine aluminium derivatives and one each of gallium and indium derivatives. Four of these structures are shown in Figure 7.

Table 2. A summary of the 27 known structures

Metal	Azine	Code	Refcode or CCDC number	Space group	Reference
B	**b**	**B*b*3**	ZUSDUM	*P*21/n	6,7
B	**a**	**B*a*3**	RAZRIT	*P*-1	8
In	**c**	**In*c*1**	SADSUL	*P*21/n	10
Al	**a**	**Al*a*1**	WECWUX	*P*-1	14
Al	**a**	**Al*a*2**	WECWEH	*C*2/c	14
Al	**a**	**Al*a*4**	WECWIL	*C*2/c	14
Al	**a**	**Al*a*5**	REWPEP	*C*2/c	15
Ga	**a**	**Ga*a*5**	REWPAL	*C*2/c	15
B	**c**	**B*c*2**	WURLUR	*P*-1	20
B	**a**	**B*a*10**	JOHXIP	*P*-1	21
B	**a**	**B*a*11**	JOHXEL	*C*2/c	21
B	**a**	**B*a*12**	JOHBIT	*P*bca	21
B	**a**	**B*a*13**	JOHBEP	$P2_1$/n	21
B	**c**	**B*c*4**	PEZVIC	$P2_1$/c	24
B	**a**	**B*a*15**	ZAZZUZ	*P*-1	27
B	**a**	**B*a*16**	ZEBBAN	*I*41/a	27
B	**a**	**B*a*17**	ZEBBER	*P*-1	27
B	**a**	**B*a*18**	GENSAX	$P2_1$/c	28
B	**a**	**B*a*19**	GENSEB	$P2_1$/n	28
B	**c**	**B*c*10**	BAYLIA	*P*ccn	31
B	**c**	**B*c*11**	BEBVOX	*C*2/c	32
B	**a**	**B*a*9**	DIXRIP	*P*-1	33
Al	**a**	**Al*a*6**	NUBREL	*P*-1	16
Al	**a**	**Al*a*7**	NUBROV	*P*-1	16
Al	**a**	**Al*a*8**	NUBSAI	$P2_1$/c	16
Al	**a**	**Al*a*9**	NUBRUB	$P2_1$/c	16
Al	**a**	**Al*a*10**	NUBRIP	*P*-1	16

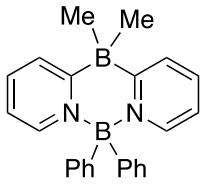

B*b*3: ZUSDUM

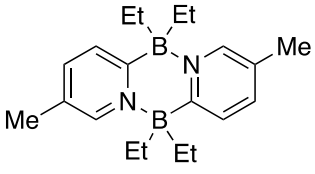

B*a*3: RAZRIT

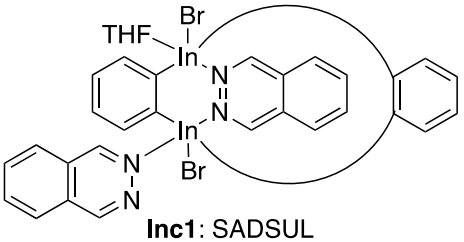

Inc1: SADSUL

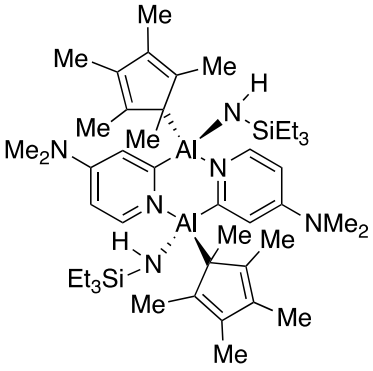

Al*a*1: WECWUX

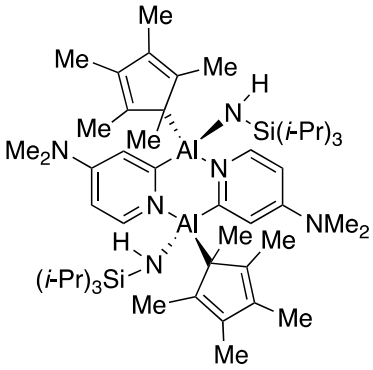

Al*a*2: WECWEH

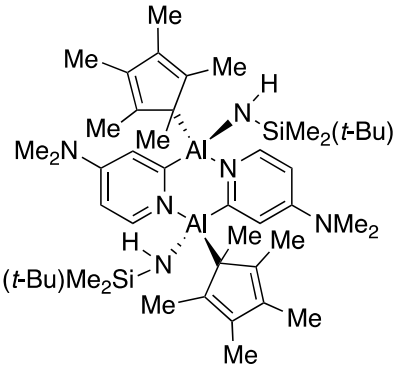

Al*a*4: WECWIL

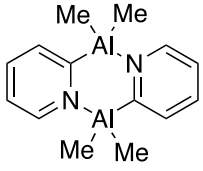

Al*a*5: REWPEP

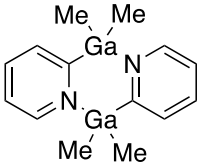

Ga*a*5: REWPAL

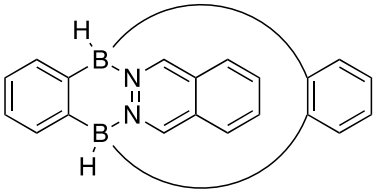

B*c*2: WURLUR

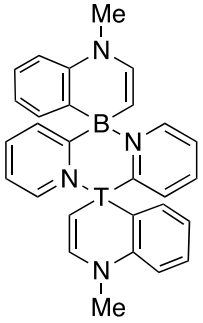

B*a*10: JOHXIP

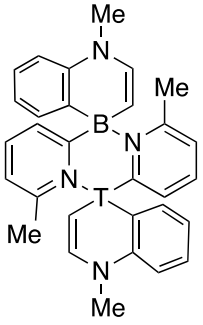

B*a*11: JOHXEL

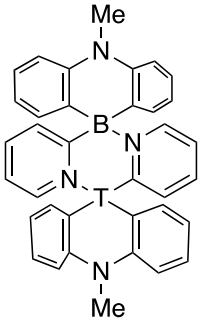

B*a*12: JOHBIT

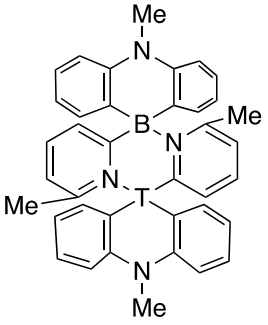

B*a*13: JOHBEP

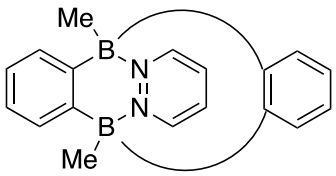

Bc4: PEZVIC

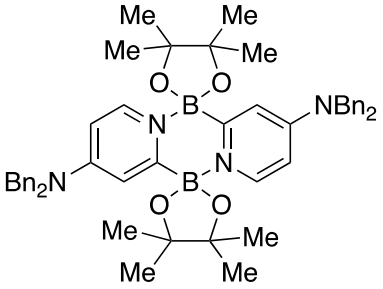

Ba15: ZAZZUZ

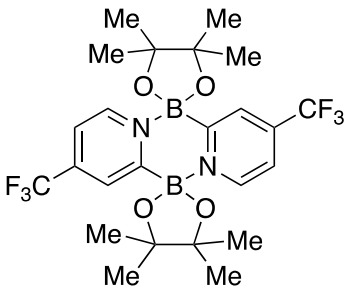

Ba16: ZEBBAN

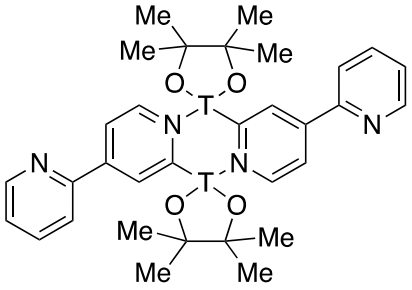

Ba17: ZEBBER

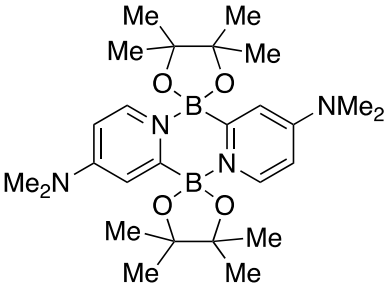

Ba18: GENSAX

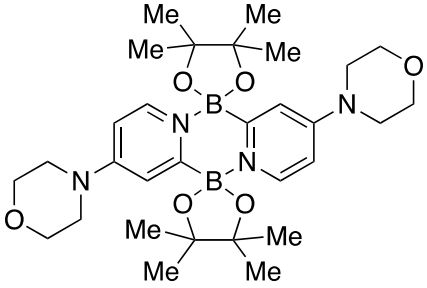

Ba19: GENSEB

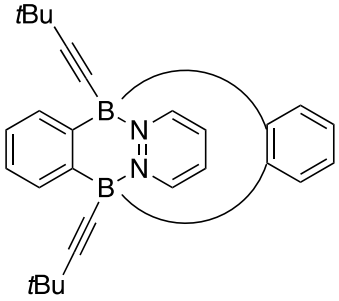

Bc10: BAYLIA

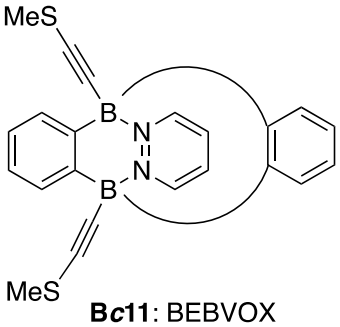

Bc11: BEBVOX

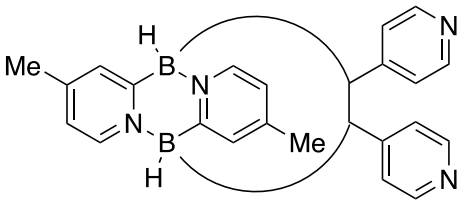

Ba9: DIXRIP

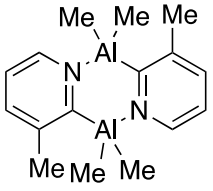

Ala6: NUBREL

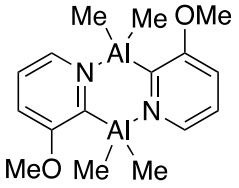

Ala7: NUBROV

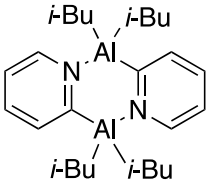

Ala8: NUBSAI

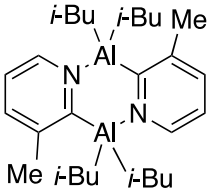

Ala9: NUBRUB

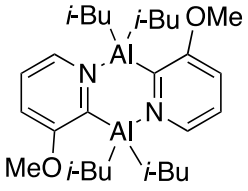

Ala10: NUBRIP

Figure 6. The 27 X-ray structures.

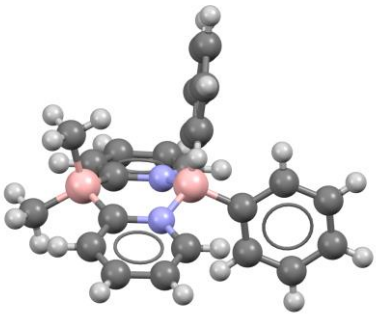

ZUSDUM **B*b*3**

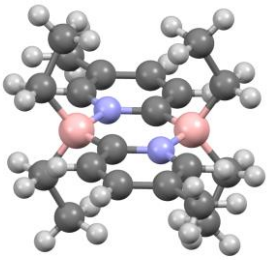

RAZRIT **B*a*3**

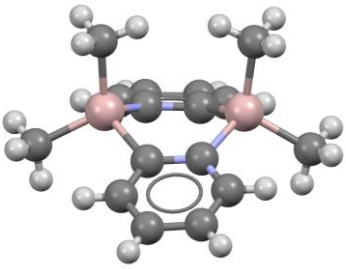

REWPEP **Al*a*5 + Al*b*5**

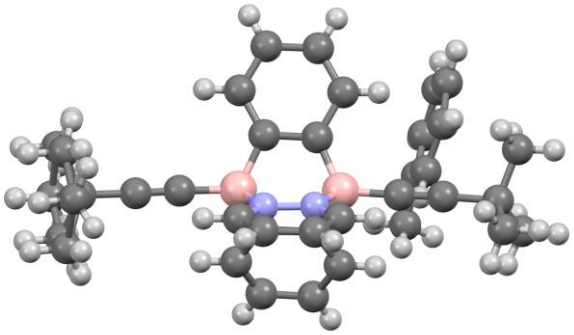

BAYLIA **B*c*10**

Figure 7. Some X-ray structures are amongst the simplest.

BAYLIA, BEBVOX and DIXRIP are Private Communications and consequently there is almost no discussion besides pure crystallographic aspects. There are other structures that are reported in the Supporting Information of the publications and are almost not examined such as WURLUR, JOHBEP, JOHBIT, JOHXEL, JOHXIP, ZAZZUZ, ZEBBAN and ZEBBER. The remaining ones have been discussed and we will summarize here these discussions.

The ZUSDUM structure,[7] for example, shows that the central ring of **B*b*3** adopts a shallow boat conformation. The B-N bonds [both 1.598(3) Å] in **B*b*3** are longer than the 1.55 Å average found in many pyrazaboles.[1] Steric effects are probably responsible for the fact that the PhBPh bond angle is wider than the MeBMe bond angle in **B*b*3**; besides, the NBN bond angle, 108.0°, is slightly narrower than the annular CBC bond angle; a "scissoring" effect caused by the bulky phenyl substituents may be responsible for this difference.

The discussion of the X-ray structure of RAZRIT[8] is very interesting. The single-crystal X-ray crystallographic study revealed the planar dimeric structure of **B*a*3** as shown in Figure 7; dihedral angles of C(2)-C(1)-N(I)-B(1) and C(4)-C(5)-N(1)-B(1) are –177.8(2)° and 178.0(2)°, respectively, and furthermore the boron atom shows a clear pyramidalization. The angles of [C(I)-B(1)-C(7)], [C(1)-B(1)-C(9)], and [C(7)-B(1)-C(9)] are 109.9(2)°, 110.7(2)°, and 109.1(2)°, respectively, which are far closer to those of the tetrahedral structure. According to the criterion proposed by Toyota and Oki,[34] the tetrahedral character (THC in %) of a boron atom correlates well to the barrier of dissociation rather than the length of the coordination bond. The THC value of the boron atom of RAZRIT is estimated to be 96.9 %. The values for **B*a*3** are 79.7 (B1) and 84.2 (B2)%, respectively. Hence, they conclude that the coordination bond of the dimer is stronger than those of a related tetramer reported in the cited paper.[8]

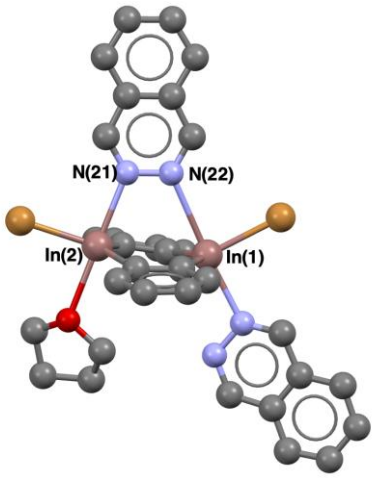

Figure 8. SADSUL, **Inc1**, without hydrogen atoms and with numbering of nitrogen and indium atoms.

The SADSUL structure, shown in Figure 8,[10] highlights the chelation of one phthalazine molecule by the diindacycle has some interesting structural aspects. The two indium atoms are displaced towards their respective coordinated nitrogen atoms N(21) and N(22), respectively. As a result the six-membered ring containing the two indium atoms has a boat-like conformation rather than being planar. The two phenylene rings of **Inc1** are not coplanar (dihedral angle of 16.5°) and the dimeric *ortho*-phenylene indium moiety adopts a saddle shape. There is one metrical parameter which merits comment. While one could question the existence of a N(22)–In(1) interaction, examination of the bond angles at In(1) and N(22) indicates clearly that N(22) is positioned at an axial site of the indium coordination sphere. Moreover, the N(22)–In(1) distance (2.446 Å) is much shorter than the sum of the van der Waals and just slightly longer than the previously reported longest In–N bond of 2.776 Å.[35] Altogether, these observations suggest the presence of a weak N(22)–In(1) dative bond.

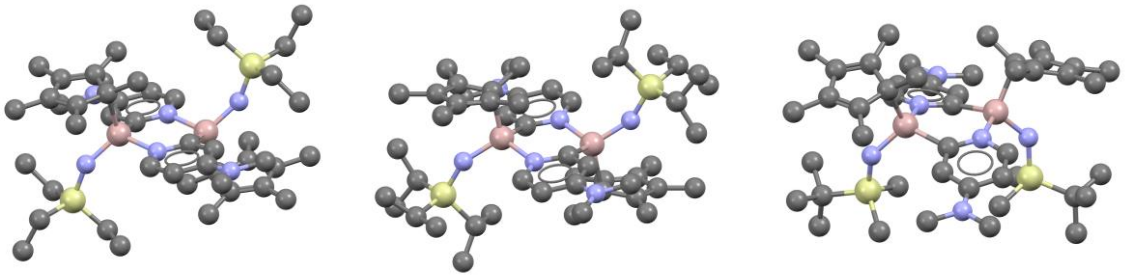

WECWUX, **Al*a*1** WECWEH, **Al*a*2** WECWIL, **Al*a*4**

Figure 9. Crystals of **Al*a*1**, **Al*a*2** and **Al*a*2** without hydrogen atoms. Si atoms in yellow.

Crystals of **Al*a*1**, **Al*a*2** and **Al*a*4** (Figure 6) were grown from solutions in toluene at –60 °C.[12] Figure 9 represent their solid-state structures. The central skeleton of WECWEH, WECWUX and WECWIL contains three six-membered rings, which adopt a dihydroanthracene-type conformation. WEXWUX and WECWEH show C_i symmetry, while WECWIL exhibits C_2 symmetry. The six-membered central rings $(AlCN)_2$ in WECWUX and WECWEH adopt a flattened chair-like conformation [degree of deformation 24.1° (**Al*a*2**), 25.3° (**Al*a*1**); 55° in cyclohexane] with the Cp* and N(H)SiRR'$_2$ groups in *transoid* orientations. The DMAP rings are in plane with the plane of the $(AlCN)_2$ chair (Figure 9), and the Cp* rings adopt a nearly coplanar orientation with respect to the central dihydroanthracene-type system. In contrast, the $(AlCN)_2$ ring of **Al*a*4** forms a distorted shell-like

conformation. The Cp* rings and N(H)Si(*t*-Bu)$_3$ groups adopt a *cissoid* orientation, due to the higher steric demand of the SiR$_3$ groups.

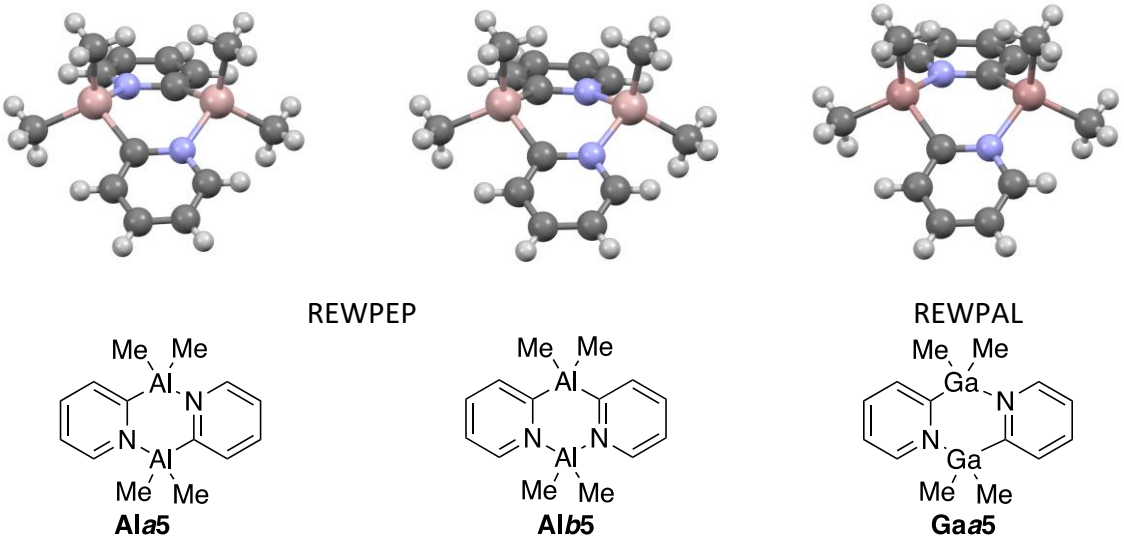

Figure 10. Structures of REWPEP (T = Al, **Al*a*5 + Al*b*5**) and REWPAL (T = Ga, **Ga*a*5**).

The X-ray structures of **Al*a*5** and **Ga*a*5** are very similar both being isomorphic.[13] These compounds are dimers consisting of boat-shaped $E_2(CN)_2$ ring units (Figure 10). The slight boat-shaped conformations of **Al*a*5** and **Ga*a*5** are similar to those found in other compounds of this review. At first sight, the **Al*a*5** and **Ga*a*5** molecules appear to exhibit a similar disorder in which each of the pyridyl ring atoms is inverted around a symmetry center in the middle-path between the two atoms of Al and Ga. This disorder results in the bridging pyridyl-C and -N atoms having a 50:50 N and C occupancy. However, according to the ^{1}H NMR data, the nature of the disorder of **Al*a*5** and **Ga*a*5** is in reality totally different. In **Al*a*5**, the pyridyl ring site disorder arises largely from the overlap of **Al*a*5** and **Al*b*5**, while in **Ga*a*5** this disorder results from the overlap of the two boat-shaped enantiomers (*i.e*. Ga–NC–Ga–NC and Ga–CN–Ga–CN). Ultimately, the result of this disruption is to make the discussion of the core E–C and E–N bond lengths and core bond angles meaningless.

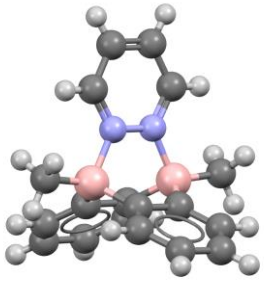

Figure 11. Structure of PEZVIC **B*c*4** (see also Figure 3).

A crystal of the air-stable Lewis acid **B*c*4** was obtained from EtOAc/BrPh 1:1 (v/v)].[24] The X-ray analysis revealed a triptycene-type arrangement (Figures 3 and 11), which was similar to a pyridazine complex of 9,10-

dihydro-9,10-diboraanthracene reported by Wegner and co-workers as well as the phthalazine complex of 5,10-dimethyl-5,10-dihydro-boranthrene.[36]

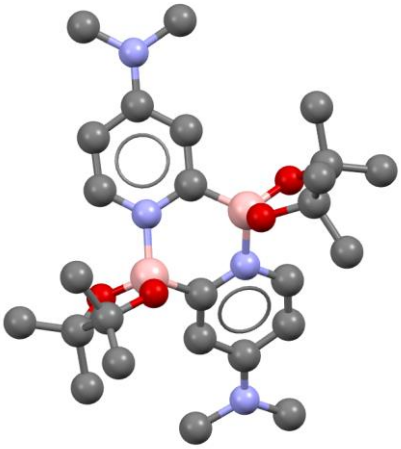

GENSAX, **B*a*18**

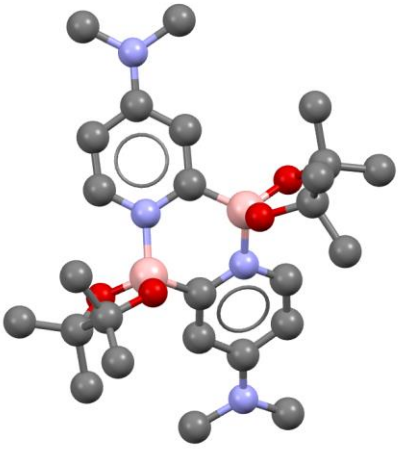

GENSEB, **B*a*19**

Figure 12. Solid-state structures of GENSAX, **B*a*18** and GENSEB **B*a*19** without hydrogen atoms.

We have depicted the structures of **B*a*18** and **B*a*19** in Figure 12[28] Note that **B*a*18** is a dimer with α-borylation regiochemistry confirmed as proposed in Scheme 22. The dimeric molecular structure of **B*a*19** was also confirmed by single X-ray diffraction, again verifying borylation in the pyridine α-position. Note also that the solid-state structures of **B*a*18** and **B*a*19** reveal that they both crystallize with the α-Bpin moieties in a *cis* arrangement and have similar bond lengths and angles (Figure 12).

Concerning the structures of Figure 4[16] the impact of the greater steric demands of the R and R' ligands can be seen directly from the solid-state structures of **Al*a*6**–**Al*a*10** (Figure 13). Whereas the previously reported dimer **Al*a*5** has a boat-shaped $Al_2(C\cdots N)_2$ ring, with a puckering angle of *ca*. 140°, the new dimers in **Al*a*6**–**Al*a*10** all have planar ring units. This change in conformation is consistent with the minimization of repulsion between the R and R' groups and/or transannular repulsion between the R groups.

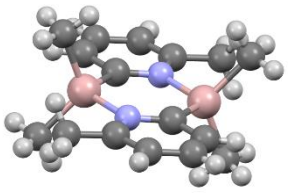

NUBREL, **Al*a*6**

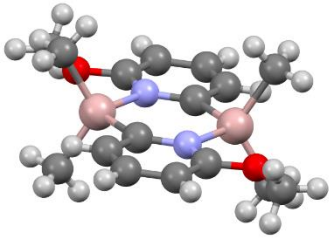

NUBROV, **Al**

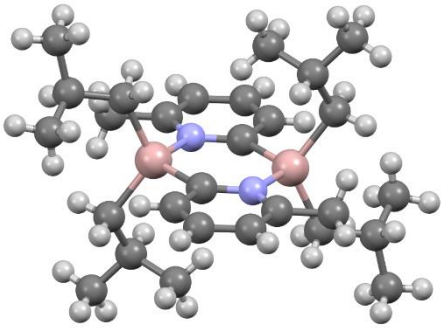

NUBSAI, **Al*a*8**

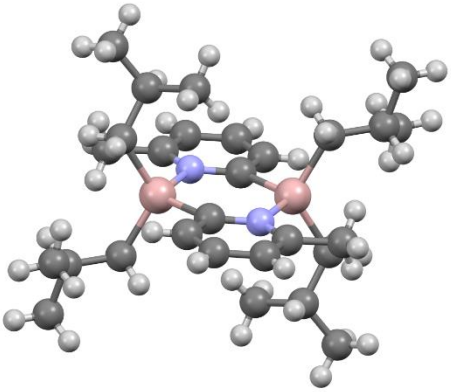

NUBRUB, **Al*a*9**

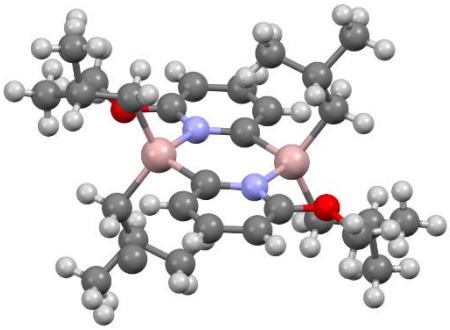

NUBRIP, **Al*a*10**

Figure 13. X-ray structures of **Al*a*6**–**Al*a*10**.

6. Theoretical Calculations

The field of theoretical calculations on the compounds of the present review was largely unexplored until Goodman, Wright *et al*. published a paper entitled *Suppressing Cis/Trans 'Ring-Flipping' in Organoaluminium(III)-2-Pyridyl Dimers – Design Strategies Towards Lewis Acid Catalysts for Alkene Oligomerization*[16] (see [15] for preliminary results). There the authors discussed one of the problems we have reported previously, the species (***a***)/1,3(***b***) isomerism, Scheme 22, or in the authors nomenclature *trans*(***a***)/*cis*(***b***) for T = Al.

The authors carried out DFT calculations at the ωB97X-D/6-311+ +G(d,p)//B3LYP-D3/6-31G(d) level of theory. Besides the 'ring-flipping' mechanism, Scheme 22, the authors considered three mechanisms (*i*) a dissociative pathway involving the formation of monomers from the *trans* isomer ***a*** which recombine into the *cis* ***b***; (*ii*) a concerted mechanism (the initially favored model) (like that depicted in Scheme 22); (*iii*) a stepwise mechanism involving Al–N bond cleavage. Mechanism (*i*) seems impossible to us.

Contrary to their initial expectations the calculations on **Al11** show that a stepwise 'swing' mechanism is the most kinetically favorable as depicted in Figure 14. The first step involves cleavage of one of the Al–N bonds of the *cis* isomer **Al*b*11** with rotation of the 2-pyridyl group in an *anti*-fashion (*i.e*. with the N-atom downwards with respect to the initial Al_2N_2 ring unit) to form an intermediate (**Al*i***) containing two four-coordinate Al atoms which then forms the new Al–N bond of the *trans* isomer ***a*** in the second step.

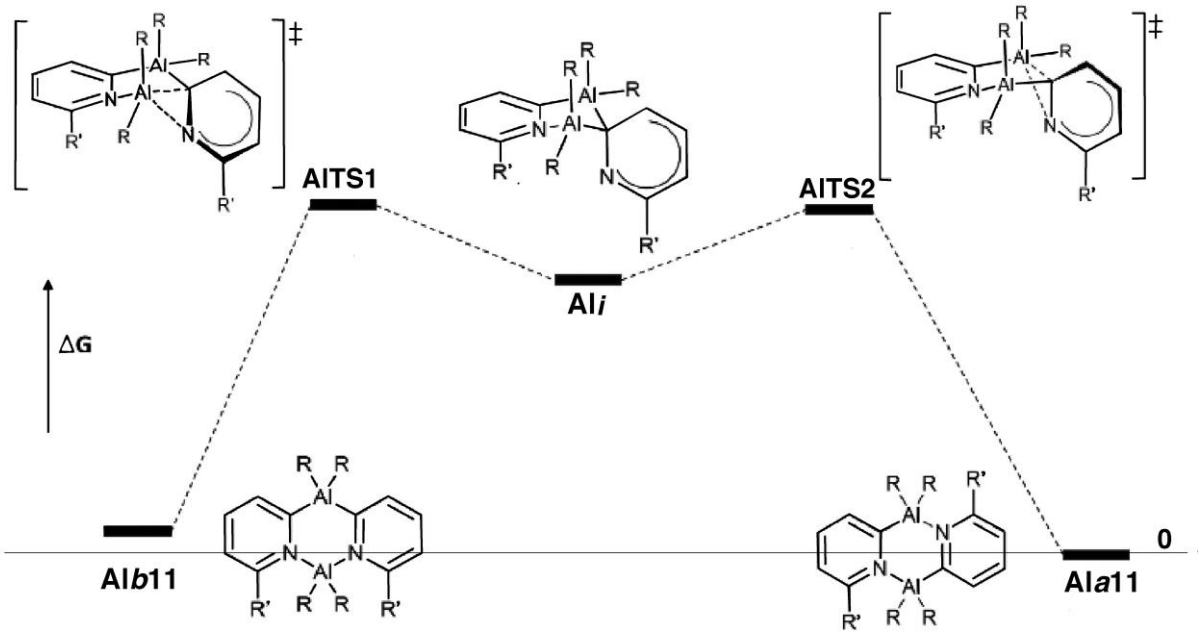

Figure 14. The stepwise mechanism involving Al–N bond cleavage.

To this mechanism corresponds the relative energies (kJ·mol^{-1}) of Table 3.

Table 3. Relative energies corresponding to DFT calculations of **Al11**

R’	R	1,3-species (***b***)	TS1	intermediate	TS2	1,4-species (***a***)
H	Me	9.2	115.1	98.7	104.6	0
Me	Me	22.6	103.3	82.8	90.8	0
H	*i*-Bu	11.3	124.7	105.4	111.3	0
Me	*i*-Bu	13.8	111.3	93.7	99.6	0

Table 3 shows a clear influence of steric factors on the thermodynamic and kinetic aspects of the reaction. Consequently, the presence of Me substituents on the 2-pyridyl rings (R' = H/Me) leads to an increase in the thermodynamic stability of the ***a*** over the ***b*** isomer presumably due to increased steric congestion in the isomer in the *N*-chelated Al-atom in the ***b*** isomer.

7. Conclusions

This review highlights the diverse synthetic methods and the critical role of regiochemistry in diazadiborinines. The reactivity of these compounds is closely related to the monomer/dimer isomerism and the “ring-flipping” mechanism. The ^{11}B NMR chemical shifts are a valuable tool for structural determination, and the 27 X-ray structures reported provide critical insights. While theoretical calculations are still in their early stages, they offer valuable guidance for understanding the behavior of these compounds.

The 6-6-6 aza-triel compounds analyzed in the present review show interesting properties, although they have been carefully explored only for boron and aluminum; the properties of gallium and indium derivatives

need to be further explored. Some aspects that deserve to be studied in the future are those related to the NMR of ^{15}N and ^{71}Ga as well as those related to the validation of the "ring-flipping" mechanism established for Al to the cases of B, Ga and In.

7. Acknowledgments

This work was carried out with financial support from the Ministerio de Ciencia, Innovación y Universidades (PID2021-125207NB-C32).

Data availability

Data sharing is not applicable to this article as no new data were created or analyzed in this study.

References

1 Nieto, C. I.; Sanz, D.; Claramunt, R. M.; Alkorta, I.; Elguero, J. *Coord. Chem. Rev*. **2022**, *473*, 214812. https://doi.org/10.1016/j.ccr.2022.214812

2 Alkorta, I.; Elguero, J. *Can. J. Chem*. **2024**, *102*, 343–354. https://doi.org/10.1139/cjc-2023-0076

3 Alkorta, I.; Ferrer, M.; Sánchez-Sanz, G.; Reviriego, F.; Elguero, J. *Struct. Chem.*, in press, 2025. https://doi.org/10.1007/s11224-024-02422-1

4 Garget, T. A.; Houston, T. A.; Kiefel, M. J.; Simone, M. I. "Bicyclic Systems with Ring Junction (Bridgehead) Boron atoms" in Comprehensive Heterocyclic Chemistry IV, Vol. 12, D. Black, J. Cossey, C. Stevens, Eds. Elsevier: Amsterdam. 2021, pp. 413-432.

5 Bubnov, Y. N., Gurskii, M., Erdyakov, S. Y. "Bicyclic Systems with Ring Junction (Bridgehead) Boron atoms" in Comprehensive Heterocyclic Chemistry III, Vol. 12, A. Katritzky, C. Ramsden, E. Scriven, R. Taylor, Eds.; Elsevier: New York, 2008; pp. 573-633.

6 Hodgkins, T. G. *Inorg. Chem*. **1993**, *32*, 6115–6116. https://doi.org/10.1021/ic00078a034

7 Hodgkins, T. G.; Powell, D. R. *Inorg Chem*. **1996**, *35*, 2140–2148. https://doi.org/10.1021/ic950775m

8 Murafuji, T.; Mouri, R.; Sugihara, Y.; Takakura, K.; Mikata, Y.; Yano, S. *Tetrahedron* **1996**, *52*, 13933–13938. https://doi.org/10.1016/0040-4020(96)00855-1

9 Taylor, S. L.; Lee, D. Y.; Martin J. C. *J. Org. Chem*. **1983**, *48*, 4158–4169. https://doi.org/10.1021/jo00170a071

10 Gabbaï, F. P.; Schier, A.; Riede, J.; Hynes, M. *Chem. Commun*. **1998**, 897–898. https://doi.org/10.1039/A800413G

11 Sopková-de Oliveira Santos, J.; Bouillon, A.; Lancelot, J.; Rault, S. *Acta Crystallogr. Section C* **2003**, *C59*, o596–o597. https://doi.org/10.1107/S0108270103016767

12 Sopková-de Oliveira Santos, J.; Bouillon, A.; Lancelot, J. C.; Rault, S. *Acta Crystallogr. Section C* **2004**, *C60*, o582–o584.

https://doi.org/10.1107/S0108270104014520
13 Bouillon, A.; Lancelot, J. C.; Sopkova-de Oliveira Santos, J.; Collot, V.; Bovy, P. R.; Rault, S. *Tetrahedron* **2003**, *59*, 10043–10049.
https://doi.org/10.1002/chin.200414183
14 Schulz, S.; Thomas, F.; Priesmann, W. M.; Nieger, M. *Organometallics* **2006**, *25*, 1392–1398.
https://doi.org/10.1021/om0509286
15 García, F.; Hopkins, A. D.; Kowenickiu, R. A.; McPartlin, M.; Silvia, J. S.; Rawson, J. N.; Rogers, M. C.; Wright, D. S. *Chem. Commun*. **2007**, 586–588.
https://doi.org/10.1039/B613748B
16 Choudhury, D.; Lam, C. C.; Farag, N. L.; Slaughter, J.; Bond, A. D.; Goodman, J. M.; Wright, D. S. *Chem. Eur. J*. **2024**, *30*, e202303872.
https://doi.org/10.1002/chem.202303872
17 Dick, G. R.; Woerly, E. M.; Burke, M. D. *Angew. Chem. Int. Ed*. **2012**, *51*, 2667–2672.
https://doi.org/10.1002/anie.201108608
18 Knapp, D. M.; Gillis, E. P.; Burke, M. D. *J. Am. Chem. Soc*. **2009**, *131*, 6961–6963.
https://doi.org/10.1021/ja901416p
19 Teltewskoi, M.; Panetier, J. A.; Macgregor, S. A.; Braun, T. *Angew. Chem. Int. Ed*. **2010**, *49*, 3947–3951.
https://doi.org/10.1002/anie.201001070
20 Lorbach, A.; Bolte, M.; Lerner, H. W.; Wagner, M. *Chem. Commun*. **2010**, 3592–3594.
https://doi.org/10.1039/C001803A
21 Xu, S.; Haeffner, F.; Li, B.; Zakharov, L. N.; Liu, S. Y. *Angew. Chem. Int Ed*. **2014**, *53*, 6795–6799.
https://doi.org/10.1002/anie.201403903
22 Schröder, J.; Himmel, D.; Böttcher, T. *Chem. Eur J.* **2017**, *23*, 10763–10767.
https://doi.org/10.1002/chem.201702890
23 Lu, Z.; Quanz, H.; Burghaus, O.; Hofmann, J.; Logemann, C.; Beeck, S.; Schreiner, P. R.; Wegner, H. *J. Am. Chem. Soc*. **2017**, *139*, 18488–18491.
https://doi.org/10.1021/jacs.7b11823
24 Hong, L.; Ahles, S.; Heindl, A. H.; Tiétcha, G.; Petrov, A.; Lu, Z.; Logemann, C.; Wegner, H. A. *Beilstein J. Org. Chem*. **2018**, *14*, 618–625.
https://doi.org/10.3762/bjoc.14.48
25 Balkenhohl, M.; Janfra, H.; Lenz, T.; Ebeling, M.; Zipse, H.; Karaghiosoff, K.; Knochel, P. *Angew. Chem. Int Ed.* **2019**, *58*, 9244–9247.
https://doi.org/10.1002/anie.201903839
26 Oeschger R. J.; Larsen, M. A.; Bismuto, A.; Hartwig. J. F. *J. Am. Chem. Soc*. **2019**, *141*, 16479–16485.
https://doi.org/10.1021/jacs.9b08920
27 Luo, Y.; Jiang, S.; Xu, X. *Angew. Chem. Int. Ed*. **2022**, *61*, e202117750.
https://doi.org/10.1002/anie.202117750
28 Rothbaum, J. O.; Motta, A.; Kratish, Y.; Marks, T. J. *J. Am. Chem. Soc*. **2022**, *144*, 17086–17096.
https://doi.org/ 10.1021/jacs.2c06844
29 Elguero, J.; Jimeno, M. L.; Nieves, R.; Ochoa, C.; Alemany, A. *J. Chem. Soc., Perkin Trans. 2* **1988**, 859–863.
https://doi.org/10.1039/P29880000859
30 Claramunt, R. M.; López, C.; Santa María, M. D.; Sanz, D.; Elguero, J. *Prog. NMR Spectrosc*. **2006**, *49*, 169–206.
https://doi.org/ 10.1002/chin.200711279

31 Lovric, I.; Bolte, M.; Wagner, M. **2022**; *CSD Communication (Private Communication*).
32 Lorbach, A.; Bolte, M.; Wagner, M. **2022**; *CSD Communication (Private Communication*).
33 Wang, Z. **2023**; *CSD Communication (Private Communication*).
34 Toyota, S.; Oki, M. *Bull. Chem. Soc. Jpn*. **1992**, *6*, 1832-1840. https://doi.org/10.1246/bcsj.65.1832
35 Bradley, D. C.; Frigo, D. M.; Harding, I. S.; Hursthouse, M. B.; Motevalli, M. *J. Chem. Soc. Chem. Commun*. **1992**, 577–578. https://doi.org/10.1039/C39920000577
36 Kessler, S. N.; Neuburger, M.; Wegner, H. A. *Eur. J. Org. Chem*. **2011**, 3238–3245. https://doi.org/10.1002/ejoc.201100335

Authors' biographies

José Elguero is *ad honorem* Research Professor at the CSIC. His research is focused on structural chemistry, hydrogen bonding, heterocyclic chemistry and NMR spectroscopy.

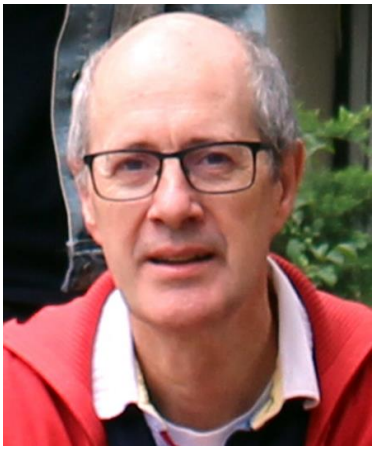

Ibon Alkorta is Research Professor at the Institute of Medicinal Chemistry of the CSIC. His main topics of research are theoretical chemistry and non-covalent interactions.